

Topology-Guided Sampling for Fast and Accurate Community Detection

FRANK WANYE, Virginia Tech
 VITALIY GLEYZER, MIT Lincoln Laboratory
 EDWARD KAO, MIT Lincoln Laboratory
 WU-CHUN FENG, Virginia Tech

Community detection is a well-studied problem with applications in domains ranging from computer networking to bioinformatics. While there are many algorithms that perform community detection, the more accurate and statistically robust algorithms tend to be slow and hard to parallelize. One way to speed up such algorithms is through data reduction. However, this approach has not been thoroughly studied, and the quality of results obtained with this approach varies with the graph it is applied to. In this manuscript, we present an approach based on topology-guided sampling for accelerating stochastic block partitioning – a community detection algorithm that works well on graphs with complex and heterogeneous community structure. We also introduce a degree-based thresholding scheme that improves the efficacy of our approach at the expense of speedup. Finally, we perform a series of experiments on synthetically generated graphs to determine how various graph parameters affect the quality of results and speedup obtained with our approach, and we validate our approach on real-world data. Our results show that our approach can lead to a speedup of up to 15× over stochastic block partitioning without sampling while maintaining result quality and can even lead to improvements of over 150% in result quality in terms of F1 score on certain kinds of graphs.

CCS Concepts: • **Information systems** → *Clustering*; • **Mathematics of computing** → **Graph algorithms**.

ACM Reference Format:

Frank Wanye, Vitaliy Gleyzer, Edward Kao, and Wu-chun Feng. 2021. Topology-Guided Sampling for Fast and Accurate Community Detection. 1, 1 (August 2021), 33 pages. <https://doi.org/10.1145/nnnnnnn.nnnnnnn>

DISTRIBUTION STATEMENT A. Approved for public release. Distribution is unlimited. This material is based upon work supported by the Under Secretary of Defense for Research and Engineering under Air Force Contract No. FA8702-15-D-0001. Any opinions, findings, conclusions or recommendations expressed in this material are those of the author(s) and do not necessarily reflect the views of the Under Secretary of Defense for Research and Engineering. Delivered to the U.S. Government with Unlimited Rights, as defined in DFARS Part 252.227-7013 or 7014 (Feb 2014). Notwithstanding any copyright notice, U.S. Government rights in this work are defined by DFARS 252.227-7013 or DFARS 252.227-7014 as detailed above. Use of this work other than as specifically authorized by the U.S. Government may violate any copyrights that exist in this work. ©2021 Massachusetts Institute of Technology.

This project was supported in part by NSF I/UCRC CNS-1822080 via the NSF Center for Space, High-performance, and Resilient Computing (SHREC).

Authors' addresses: Frank Wanye, wanyef@vt.edu, Virginia Tech, 620 Drillfield Drive, Blacksburg, Virginia, 24061-0217; Vitaliy Gleyzer, vglyzer@ll.mit.edu, MIT Lincoln Laboratory, 244 Wood Street, Lexington, Massachusetts; Edward Kao, edward.kao@ll.mit.edu, MIT Lincoln Laboratory, 244 Wood Street, Lexington, Massachusetts; Wu-chun Feng, wfeng@vt.edu, Virginia Tech, 620 Drillfield Drive, Blacksburg, Virginia, 24061-0217.

Permission to make digital or hard copies of all or part of this work for personal or classroom use is granted without fee provided that copies are not made or distributed for profit or commercial advantage and that copies bear this notice and the full citation on the first page. Copyrights for components of this work owned by others than ACM must be honored. Abstracting with credit is permitted. To copy otherwise, or republish, to post on servers or to redistribute to lists, requires prior specific permission and/or a fee. Request permissions from permissions@acm.org.

© 2021 Association for Computing Machinery.

XXXX-XXXX/2021/8-ART \$15.00

<https://doi.org/10.1145/nnnnnnn.nnnnnnn>

1 INTRODUCTION

Data from a wide variety of sources, including domains such as bioinformatics [38], the world wide web [15], and computer networks [20], can be represented as graphs. In this representation, individual entities are represented as graph vertices, and the relationships between them are represented as edges. These edges can be directed or undirected as well as weighted or unweighted.

In real-world graph data, it is often possible to group vertices into communities such that vertices within a community are more strongly connected to each other than they are to vertices outside their community. These communities can either be non-overlapping, where a single vertex belongs to at most one community, or overlapping, where a single vertex belongs to more than one community. This grouping process is known as community detection.

Community detection has a multitude of applications in a variety of domains. In computational clusters, community detection can be used to reduce the communication overhead when assigning workloads to computational nodes [23]. In biological networks, identifying communities of protein interactions can help with the identification of functional modules [38]. It has also been shown to improve the accuracy of classification tasks [24, 42] and to help inform the placement of servers in communication networks [20].

However, optimal community detection is an NP-hard problem [5], making it intractable for real-world graphs, which can consist of billions of vertices and edges. As such, a number of sub-optimal approaches have been developed to facilitate community detection on large graphs. These approaches are based on heuristics such as minimum cut, vertex similarity, modularity maximization, and statistical inference [5].

Of the aforementioned heuristics, modularity maximization, where vertices are grouped into communities to maximize the number of edges between vertices in the same communities, is a commonly applied heuristic [17] due to its relative speed and scalability [2]. The popularity of modularity maximization has also led to substantial work into parallel and distributed implementations of algorithms based on this heuristic [9, 10, 12, 26, 40]. However, modularity maximization has a resolution limit that limits the size of the communities that can be detected with these methods [6, 33] and affects the quality of results achieved when they are applied to graphs where the community sizes vary widely.

To address the above issues, we propose and design a data-sampling approach based on the stochastic block partitioning (SBP) algorithm [33, 34]. SBP is a statistical inference-based algorithm for performing non-overlapping community detection on unattributed graphs. SBP has a relatively low algorithmic complexity of $O(|E| \log^2 |E|)$ in terms of the number of edges $|E|$ in the graph. Furthermore, it does *not* suffer from the resolution limit because it is *not* based on the modularity metric [17]. More importantly, SBP is robust on graphs where the community sizes vary widely and the connectivity between the communities is high, making it especially desirable for graphs where communities are hard to detect. However, it suffers from scalability issues, making its serial implementation infeasible for large graphs. Additionally, the algorithm is based on an inherently serial inference technique, making parallelization nontrivial [17].

Several attempts have been made to improve the runtime of the SBP algorithm, including via graph streaming [45] and distributed processing on computational clusters [46]. The streaming approach seeks to speed up community detection by streaming the graph in batches. Our approach complements the above by focusing on data reduction for accelerating SBP. Combining our approach with either of the above approaches would lead to further speedup gains.

Our proposed data-sampling approach for accelerating SBP and, in turn, community detection in general, has been shown to work well on synthetically generated graphs [49]. However, these prior results show performance variations on different graph inputs, variations that have not

yet been explainable. Additionally, our approach has not been tested on real-world data. In this manuscript, we tackle both of these issues. That is, we conduct several experiments on synthetic graphs generated in a manner that allows us to study the effects of several graph parameters on the performance of our approach, and we evaluate our approach on many real-world web graphs. Although we use SBP exclusively in this work due to its aforementioned strengths, we stress that our approach can be easily utilized to accelerate any community detection algorithm.

Our main contributions are as follows:

- A data sampling approach for speeding up stochastic block partitioning, a community detection algorithm that is robust to complex and heterogeneous community structure in real-world graphs.
- A degree-based thresholding scheme to augment existing sampling algorithms in order to better preserve the quality of results from community detection.
- An empirical study of the computational gains and result quality with our sampling approach on synthetically generated graphs with varying properties.
- A detailed evaluation of the overall efficacy of our approach on a combination of synthetic and real-world data.

Overall, we show that our approach can lead to speedups of up to $15\times$ while maintaining result quality at comparable levels to stochastic block partitioning without sampling. On some graphs, it can even improve result quality by upwards of 100% (see Fig. 1). We attribute this improvement in quality to the effect that search-space reduction via sampling has on SBP.

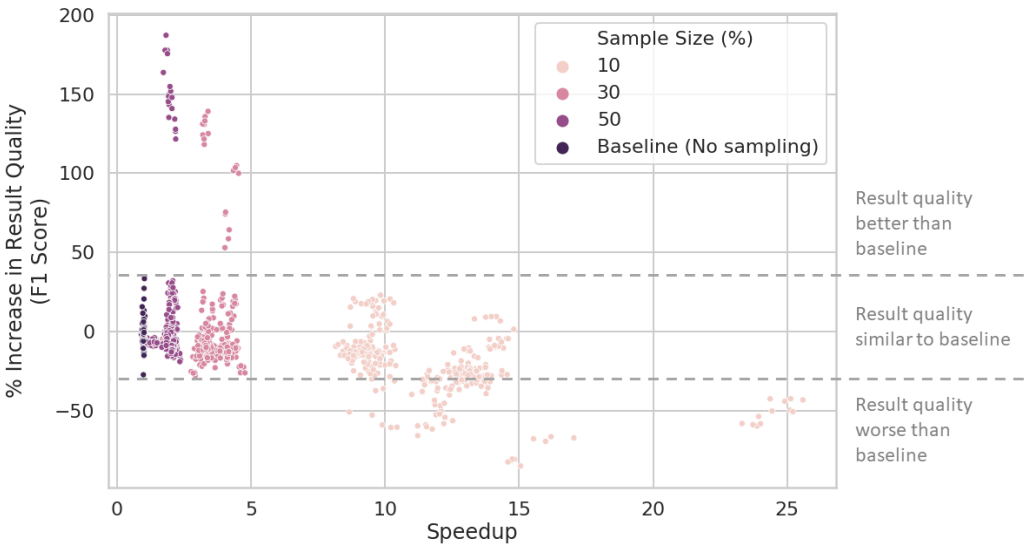


Fig. 1. Trade-off between result quality and speedup with our sampling approach on a set of realistic synthetic graphs (see §4.3) using the best-performing sampling algorithms (see §5.2). Each point represents one run with a particular combination of sample size, sampling algorithm, and graph. Metrics are calculated against the average baseline result on a per-graph basis. The results from the baseline algorithm runs demonstrate the variation in result quality that is inherent to stochastic block partitioning. We achieve a speedup up to just under $15\times$ without significantly affecting the result quality. Alternatively, we achieve greater than 150% improvement in result quality on certain graphs at a more modest speedup.

2 RELATED WORK

In this section, we introduce existing research related to graph generation, community detection, accelerating community detection, and sampling from graphs.

2.1 Stochastic Blockmodels

Stochastic Blockmodels (SBMs) are a set of graph models that can be used to generate and perform inference on graphs. They represent the graph as a matrix of probabilities of edges existing between communities. The simplest SBM is a matrix $B \in \mathbb{R}^{C \times C}$, where C is the number of communities represented in the blockmodel, and $B_{i,j}$ is the probability of any given edge being between a vertex in community i and a vertex in community j . Given that n_i and n_j refer to the number of vertices in communities i and j , respectively, how well a blockmodel represents a given graph G can be calculated using the unnormalized log-likelihood of the graph given the model via the following equation [19]:

$$L(G|B) = \sum_{i,j} B_{i,j} \ln \left(\frac{B_{i,j}}{n_i \cdot n_j} \right). \quad (1)$$

This simple model, however, assumes degree heterogeneity between the vertices in the graph, and thus fails to accurately model real-world data. The Degree-Corrected SBM (DCSBM) addresses this assumption. In the DCSBM, the probability of an edge between two vertices, v_i and v_j in communities i and j , respectively, also depends on the degrees of v_i and v_j . Given that $e_{i,out}$ refers to the total number of outgoing edges from the vertices in community i , and $e_{j,in}$ is the total number of incoming edges to the vertices in community j , the unnormalized log-likelihood of the graph G given the DCSBM is calculated via the following equation [19]:

$$L(G|B) = \sum_{i,j} B_{i,j} \ln \left(\frac{B_{i,j}}{e_{i,out} \cdot e_{j,in}} \right). \quad (2)$$

The above formulation is parametric in the sense that the number of communities making up the blockmodel B needs to be known beforehand. Given that $M_{k,l}$ is the adjacency matrix term corresponding to vertices v_k and v_l , $d_{k,out}$ and $d_{k,in}$ refer to the out- and in-degree of vertex v_k , respectively, the nonparametric log-likelihood of the DCSBM is calculated via the following equation [37]:

$$L(G|B) = \ln \left(\frac{\prod_{i,j} B_{i,j}!}{\prod_i e_{i,out}! \prod_i e_{i,in}!} \times \frac{\prod_k d_{k,out}! \prod_k d_{k,in}!}{\prod_{k,l} M_{k,l}!} \right). \quad (3)$$

For a derivation of Equation 3, we refer the reader to [37].

2.2 Graph Generation

Graph generation is an important aspect of evaluating community detection methods due to the scarcity of real-world graph data with known communities. As such, it is a well-studied problem with several solutions. The simplest graph generators are based on simple probabilistic rules. Erdős-Rényi [4] random graphs, for example, are generated such that there is a uniform probability of an edge being present between any two vertices. However, graphs generated in this fashion do not have an explicit community structure.

Generative models such as the planted l -partition solve this problem by using one probability for edges between vertices in the same community and another for those in different communities, but do not account for variation in degree distributions between communities [3]. The Lancichinetti-Fortunato-Radicchi (LFR) [21] benchmark improves upon this by modeling both the distributions of

vertex degrees and community sizes as power law distributions, and then using a mixing parameter to control the proportion of each vertex's edges that fall within its community. This model, however, forces all vertices to have the same percentage of edges fall within their own community. A different approach is to generate graphs based on a variant of the SBM [19]. Here, a blockmodel is defined first, and the edges are then added to fit the blockmodel description. This approach allows for more flexibility than the LFR benchmark with respect to control over the graph parameters.

2.3 Stochastic Block Partitioning

Several methods for performing community detection exist in the literature. Modularity-maximization methods like the Louvain method [2] agglomerate subgraphs into larger structures based on the resulting gain in modularity. Message-passing algorithms like label propagation [41] propagate community membership information from vertex to vertex. Spectral clustering methods [31] use matrix decomposition techniques to generate low-dimensional embeddings for vertices, which are then clustered using k-means. Statistical inference methods tend to optimize some optimality metric based on probabilistic graph models such as the Community-Affiliation Graph Model [51] or the Stochastic Blockmodel (SBM) [19]. Recently, graph neural networks have also been used to perform community detection in graphs [16, 28, 39].

The Stochastic Block Partitioning (SBP) [17, 34, 35] algorithm is an iterative, agglomerative statistical inference method for community detection, based on inference over the Degree-Corrected Stochastic Blockmodel (DCSBM) [37]. This inference can be done by minimizing the entropy of the blockmodel, but because the blockmodel has the lowest entropy when $|C| = |V|$, that only works when the number of communities is known beforehand. In order for the model to be able to discover the optimal number of communities, the SBP algorithm minimizes the minimal description length H of the DCSBM, which represents the total amount of information needed to describe the blockmodel itself. Given a graph G consisting of $|E|$ edges and $|V|$ vertices, described by a blockmodel with $|C|$ communities, H is given by [37]:

$$H = -\ln(B) - L(G, B), \quad (4)$$

where $L(B|G)$ is computed using Eq. (3) and $\ln(B)$ is computed as follows:

$$\ln(B) = \sum_i \ln |C_i|! - \ln \left(\binom{|C|(|C|+1)/2}{|E|} \right) - \ln \left(\frac{|V|-1}{|C|-1} \right) - \ln |V|! + \ln \left(\prod_i \frac{\prod_d |v_d^i|!}{|C_i|} \prod_i q(e_i, |C_i|)^{-1} \right), \quad (5)$$

where $\binom{n}{m} = \frac{n!}{m!(n-m)!}$, $\binom{n}{m} = \frac{n!}{m!(n-m)!}$, $|v_d^i|$ is the number of vertices in block i with degree d , $|C_i|$ is the number of vertices in block i , and $q(n, m)$ refers to the ‘‘number of restricted partitions of integer a into at most b parts’’. For a more in-depth discussion of H , we refer the reader to [37].

Initially, each vertex is treated as a separate community. Each iteration of the algorithm consists of two phases. In the first phase, communities are merged together based on the resulting difference in H . In the second phase, the community memberships are fine-tuned at the vertex level using the Metropolis-Hastings algorithm [14]. By keeping up to three copies of the DCSBMs obtained with different numbers of communities, a search can be performed to find the optimal number of communities and the optimal DCSBM for this number of communities. The algorithm is visually summarized in Figure 2.

Although this algorithm is slower and harder to parallelize than several alternatives, we focus on it because of its robustness to (a) high variation in community sizes and (b) complex community structure as characterized by high intercommunity connectivity in real-world graphs. This is corroborated by comparing the results obtained by SBP [9, 49], Fast-Tracking Resistance [9], Louvain [9, 11], and Label Propagation [25] on the Graph Challenge [17] datasets. Across all those

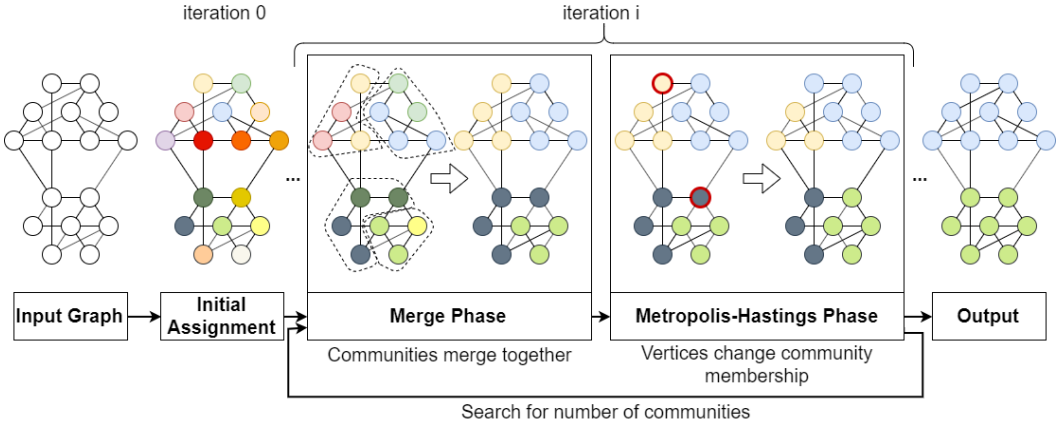


Fig. 2. Snapshots of a graph at various stages of the stochastic block partitioning algorithm.

implementations, SBP delivered the best and most consistent performance on graphs with complex and heterogeneous structure. Furthermore, running the graph-tool SBP implementation [36] on the same graphs led to even better results than those reported in [9, 49].

2.4 Accelerating Community Detection

Much of the research into accelerating community detection algorithms has centered around modularity maximization algorithms like Louvain and fast heuristics such as label propagation, which have been parallelized on multi-core [13, 26], multi-node [9, 12, 25, 40], and heterogeneous architectures [30].

Speeding up the SBP algorithm is challenging and has not received as much research attention. Although the first phase of the algorithm, where communities are agglomerated, is embarrassingly parallel, the second phase, where individual vertices move between communities, poses many challenges. These challenges arise because the Metropolis-Hastings algorithm is an inherently serial Markov Chain Monte-Carlo (MCMC) method. Every time a move is accepted, the DCSBM changes, which affects the probabilities of all subsequent vertex moves being accepted or rejected. Parallelizing such MCMC algorithms is an open problem, with different challenges arising depending on how the algorithm is parallelized [50].

Furthermore, partitioning the graph across multiple computational nodes in a distributed setting is difficult because changes in community membership need to be communicated to all neighboring vertices, which may reside on different computational nodes. Optimally partitioning the graph to reduce communication is *not* viable due to high computational costs. In [46], a distributed SBP implementation is proposed where the graph is randomly partitioned between computational nodes. Each node runs SBP on an independent subgraph and then the independent results are heuristically merged. Within each node, a single aggregator thread is used to batch vertex communication. While promising, the aggregator thread being responsible for all communication can lead to a performance bottleneck, while batching communication reduces the accuracy of results by forcing the probability computation to use stale DCSBM parameters. Additionally, a random partition of the graph is likely to break the graph structure when the number of partitions is large (or conversely, when the partitions are small), which could have an effect on the final community detection results.

Our approach leverages an existing partially parallelized implementation of SBP, while focusing on delivering further speedup gains through data reduction.

2.5 Data Reduction in Graphs

Reducing the size of graphs before storing or processing is a common technique, including agglomerative approaches that combine multiple vertices into a single super-node [44], selective edge deletion [1], task-driven subgraph discovery [29], and various sampling techniques [1, 22, 27, 48]. In this work, we focus on vertex-sampling techniques for their relative simplicity and because removing a vertex from a graph also removes the edges connected to it, thus reducing the size of the graph along both the vertex and edge dimensions.

Graphs have a multitude of properties that describe the graph, including the graph diameter, vertex degree distribution, sparsity, strongly connected components, and clustering coefficient. A "perfect" data reduction scheme would preserve all of these properties. Unsurprisingly, this is an impossible task with sampling. Studies into sampling algorithms [1, 22, 27, 48] show that different sampling algorithms excel in preserving different subsets of a graph's properties, with no one algorithm consistently performing well across all properties.

Traditional graph sampling algorithms have been previously studied in the context of community detection. The ability of uniform random edge sampling to preserve community structure in graphs was tested in [7], but the community memberships of vertices not present in the sample were not inferred. Our preliminary work [49] also compares several traditional sampling algorithms for the purpose of speeding up the SBP algorithm. The results of these experiments suggest that, given a large enough sample size, even simple random sampling algorithms can preserve community structure. However, the quality of the final community detection results in [49] varied greatly across the different graphs, sample sizes, and sampling algorithms tested, suggesting that some latent factors greatly influence the ability of sampling algorithms to preserve community structure.

Other sampling algorithms are developed specifically to preserve the graph's community structure. To the best of our knowledge, there is no known metric of community structure which can be calculated without knowledge of the community memberships of the graph's vertices. However, a related metric called Expansion Factor (EF) was proposed [27], which measures the number of vertices adjacent to the sample as a fraction of the number of vertices in the sample. The higher the EF, the more of the graph the sample explores, leading to a higher likelihood of including vertices from every community. New sampling algorithms based on the EF metric were also developed. When these algorithms were applied to the community detection problem, they showed promising results for inferring the community structure of vertices *not* present in the sample [27]. We include one of these algorithms in our experiments (See §3.3).

Our work builds on top of the approach introduced in [49] and extends it with a thresholding scheme based on vertex degree, which improves the quality of obtained community detection results at the expense of some speedup.

3 SAMPLING METHODOLOGY

In this section, we describe our four-step sampling methodology, motivate our proposed thresholding strategy, and present the sampling algorithms we chose for testing and evaluation.

3.1 Approach

We propose a four-step approach (illustrated in Figure 3) to accelerate community detection using sampling. Given a graph G containing the set of vertices V and edges E , a community detection algorithm run on G produces a vertex-to-community assignment vector A . The goal of our approach is to perform community detection on a sampled graph G^S and then extend the results to G , producing a vertex-to-community assignment A^S such that it is of similar quality to A , in a much shorter amount of time. We adopt two measures of quality for A - F1 Score for synthetic

graphs where the true communities are known (see §5) and Quality Score for real-world graphs where the true communities are not known (see §6.1).

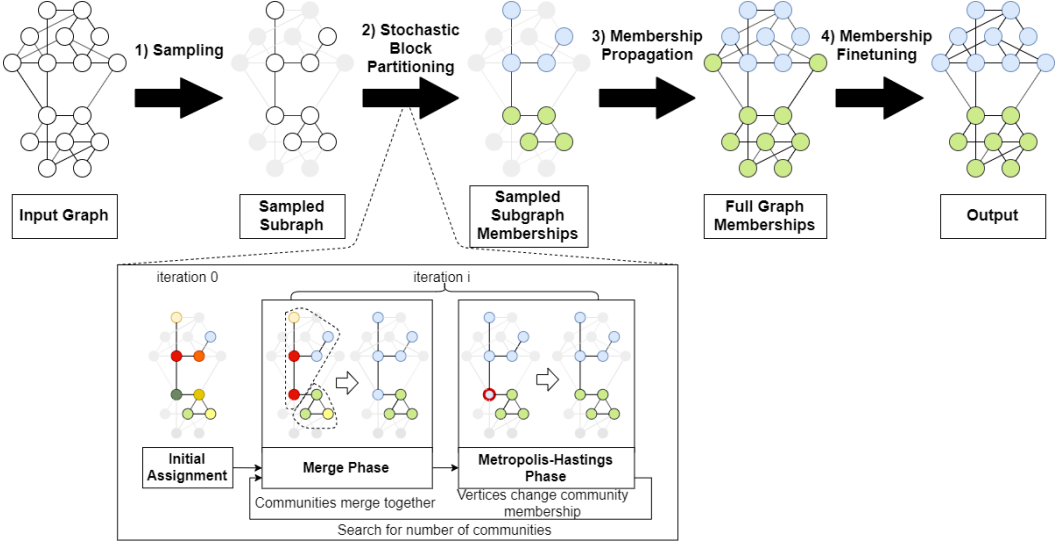


Fig. 3. An illustration of our sampling approach for community detection.

The four steps of our approach are outlined below:

- (1) A sampling algorithm is used to select V^S , a subset of vertices from the full graph. The sampled graph G^S is then generated by adding only the edges that exist between vertices in V^S .
- (2) Stochastic block partitioning (described in Figure 2) is applied to G^S , obtaining a community membership for every vertex in V^S . Because community detection algorithms tend to have superlinear computational complexities, we expect the time taken to perform community detection on G^S to decrease by a factor larger than $\frac{|V|}{|V^S|}$. This step can be replaced with any other non-overlapping community detection algorithm, including a distributed implementation of SBP.
- (3) The resulting community assignments for V^S need to be propagated to the entire set of vertices V . First, the community membership of a vertex in V is set to the community to which it has the most outgoing edges. Then, if the vertex is not directly connected to any vertices in V^S , a random community is assigned to it.
- (4) Because the above propagation step can lead to a sub-optimal A^S , the community memberships of V are further fine-tuned via a non-agglomerative vertex-level algorithm to produce the final vertex-to-community assignment A^S .

This approach is heavily reliant on the quality of the sample on which community detection is run. A sample that does not preserve community structure will lead to poor vertex-to-community assignments for V^S , which will in turn lead to a low quality A^S . For this reason, the choice of sampling algorithm and sample size is very important. We explore these choices in §5.2.

3.2 Thresholded Sampling

Previous work has shown that sampling can preserve community structure as well as allow for the structure to be inferred for unsampled vertices [27, 49]. However, the graphs used in those efforts

are much denser than the graphs we target in this manuscript. These differences naturally suggest that the sampling strategies that perform best on web graphs differ from the more dense graphs in previous work because low-density graphs present a unique challenge for sampling. Lower graph densities imply that the degree distribution of the graph is skewed towards the low end. As such, it is much more likely to lead to vertices with low degrees being selected in the sample. This presents a problem because the community-related information content of an edge is proportional to the vertex degrees of the two vertices connected by said edge [18]. If the sampled subgraph contains more low-degree vertices, then the total information content of the edges in this subgraph will be comparatively low. Island vertices would provide absolutely no useful information.

To counteract this effect, we propose a simple thresholding scheme, where vertices are only considered for a sample if their vertex degree is above a threshold t . This ensures that only higher-degree vertices are included in the sample and increases the chances that a vertex has multiple edges in the sample itself, thereby increasing its information content.

3.3 Sampling Algorithms

We choose five sampling algorithms for testing our sampling approach, based on their performance in previous work [22, 27, 49] and on our thresholded sampling concept. These algorithms include an entirely random algorithm (i.e., uniform random sampling) and algorithms that are guided by the topology of the graph (i.e., random node neighbor sampling, forest fire sampling, expansion snowball sampling, and maximum degree sampling), as shown in Figure 4. The random algorithms are free of bias, while the topology-guided algorithms aim to capture different properties of the graph.

3.3.1 Uniform Random Sampling (UR). The UR algorithm [22] is the simplest of the five. The target number of vertices is selected from the graph, with each vertex having an equal probability of being selected. This leads to very fast, unbiased sampling. However, due to the random nature of UR sampling, the results are unstable; certain regions of the graph may remain unexplored or under-explored, and sampled vertices may be disconnected from the rest of the sample. Despite these drawbacks, it has been shown to outperform several exploration-based algorithms in preserving community structure [49] at larger sample sizes.

3.3.2 Random Node Neighbor Sampling (RNN). The RNN algorithm [22] is an extension of UR sampling. We classify it as one of the topology-guided algorithms because it aims to capture vertex neighborhoods. Initially, a set of seed vertices is selected in the same manner as in UR sampling. Then, the algorithm loops over the seed vertices, adding the seed vertex and all the neighbors that can be reached by outgoing edges from the seed vertex to the sample, until the target number of vertices is reached. Like UR sampling, it is fast and unbiased as well as more stable, in the sense that it is highly unlikely for a vertex to be completely disconnected from the rest of the sample. It is also likely to produce denser sampled graphs than the other algorithms. There is still a chance of inducing multiple small disconnected components, which could negatively impact community detection. This algorithm has been shown to preserve community structure well [49], especially at smaller sample sizes.

3.3.3 Forest Fire Sampling (FF). The FF algorithm [22] is another topology-guided sampling algorithm based on probabilistic exploration of the graph. Starting from a randomly selected seed vertex, outgoing neighbors are probabilistically sampled using a geometric distribution with $p = 0.7$ (as in [22]). Outgoing neighbors that were not selected are marked as visited. Vertices that were selected are added to the sample and serve as the new frontier. The algorithm is then repeated, this time using all vertices in the frontier as seed vertices. This is repeated until the target number of vertices

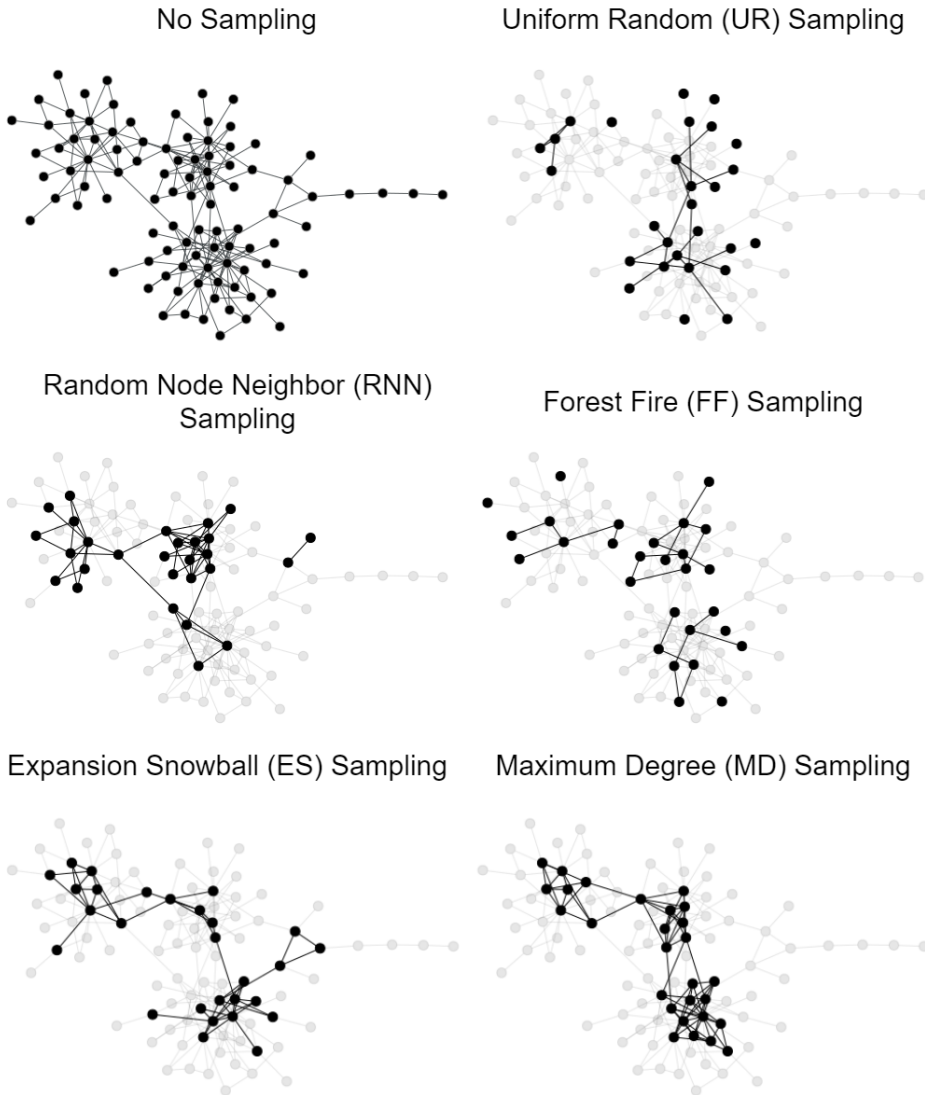


Fig. 4. Visual representation of 30% samples of the same undirected graph using the uniform random, random node neighbor, forest fire, expansion snowball and maximum degree sampling algorithms, without thresholding.

is reached, or the algorithm gets stuck, at which point it is restarted from an unvisited vertex. FF sampling is highly likely to explore as much of the graph as is possible with the given sample size. It performs comparably to UR sampling [49] at preserving community structure. However, it should be noted that different values of p could change the performance of the algorithm.

3.3.4 Expansion Snowball Sampling (ES). The ES algorithm [27] is a non-probabilistic exploration-based sampling algorithm, based on the concept of the Expansion Factor (EF). The algorithm keeps track of both the vertices in the current sample and the neighbors of the sample (vertices linked to the sample by outgoing edges). At each step, the vertex that leads to the highest increase in the sample's EF is selected, by selecting the vertex that contributes the most new neighbors to the sample. This selection step makes the algorithm a topology-guided one. These calculations make ES sampling more computationally expensive than the remaining algorithms, but it has been shown to produce good results which can be extended to the full graph [27].

3.3.5 Maximum Degree Sampling (MD). The MD algorithm is a natural extension of the thresholded sampling approach and the ES topology-guided algorithm and aims to capture the most informative vertices. If vertices with high degrees contribute the most community-related information to the sample, then naturally, the best sampling strategy would be one that simply samples the vertices with the highest degrees. However, this method is likely to produce sampled graphs with a very different structure from the original graph, which intuitively should limit the quality of community detection results obtained with this algorithm. Good performance with this algorithm would suggest that vertex degree is the most important vertex property related to community structure.

4 EXPERIMENTAL SETUP

In this section, we describe the graphs used for our experimental study as well as the hardware and software used to run these experiments.

4.1 Real-World Graphs

From the Network Data Repository [43], we select a set of 10 web graphs based on the wide range of properties they exhibit, where vertices represent webpages and edges represent links between them. Like most real-world scenarios, the true community memberships for vertices in these graphs is unknown. We describe our solution to evaluating community detection results on these graphs in §6.1.

Table 1 presents the selected graphs.

Table 1. Selected real-world graphs.

| ID | Name | Directed? | Number of Vertices $ V $ | Number of Edges $ E $ |
|-----|-------------------------|-----------|--------------------------|-----------------------|
| R1 | web-NotreDame | True | 325729 | 1497134 |
| R2 | web-arabic-2005 | False | 163598 | 1747269 |
| R3 | web-Stanford | True | 281903 | 2312497 |
| R4 | web-italycnr-2000 | True | 325557 | 3216152 |
| R5 | web-baidu-baike-related | True | 415641 | 3284387 |
| R6 | web-wikipedia2009 | False | 1864433 | 4507315 |
| R7 | web-google-dir | True | 875713 | 5105039 |
| R8 | web-it-2004 | False | 509338 | 7178413 |
| R9 | web-BerkStan-dir | True | 685230 | 7600595 |
| R10 | web-uk-2005 | False | 129632 | 11744049 |

4.2 Graph Generator

To aid in the evaluation of our sampling approach, the graphs we generate need to have the following characteristics:

- *a known and discernible community structure* to ensure that running community detection on these graphs produces meaningful results, whose quality can be easily measured
- *similarity to real-world graphs* to ensure that our analysis of them is pertinent to real-world data
- *parameters that vary in such a way as to minimize interactions* to ensure that the effects of individual parameters can be isolated and studied

To satisfy these requirements, we generate directed graphs based on the DCSBM [19] using the graph-tool software library [36], similar to those generated for the IEEE/Amazon/MIT Streaming Graph Challenge [17]. This ensures that the vertex community memberships are known and that the graph has a well-defined community structure.

In generating our graphs, we vary the following six parameters:

- (1) **Number of vertices ($|V|$):** The number of vertices $|V|$ in the graph is controlled by the size of the community membership array, which is a user-provided parameter to the graph generation function. Due to the stochastic nature of the DCSBM-based graph generator, some vertices end up as islands, i.e., zero incoming and outgoing edges. To compensate for this, we generate 113% of the target number of vertices and then filter out the island vertices.
- (2) **Number of communities ($|C|$):** In this work, we only consider the case of non-overlapping communities $|C|$. Hence, the number of communities is much lower than the number of vertices in the graph.
- (3) **Standard deviation of community sizes (σ):** The communities in a graph are rarely of the same size. The degree to which the sizes of the communities differ is highly likely to affect the results of community detection, as large communities may absorb smaller ones, or conversely, be broken up into smaller communities. Poor sampling techniques may exacerbate this problem. We control the standard deviation of community sizes σ indirectly by sampling the community membership array from a parameterized Dirichlet distribution.
- (4) **Strength of community structure (s):** We define the strength of community structure s as the ratio of the number of edges within communities to the number of edges between communities. This parameter is controlled by manually generating the blockmodel from which the graph will be generated. We first generate a blockmodel B such that $B_{i,j} = 1$ if $i = j$, and $\frac{1}{x(|C|-1)}$ otherwise, where x is a user-defined parameter; as x increases, the more the edges are concentrated within communities. In order to ensure the number of edges to and from a community is proportional to its size, we scale B such that $B_{i,j} = B_{i,j} * |C_i| * |C_j|$, where $|C_i|$ and $|C_j|$ are the sizes of the communities i and j , respectively.
- (5) **Strength of high-degree vertices (d^{max}):** We control the strength of high-degree vertices using a single value, which is the maximum vertex degree d^{max} that can be sampled from the power-law degree distribution without changing the power-law exponent. For the same reasons as above, our control of d^{max} in the generated graph is indirect.
- (6) **Density (ρ):** We measure the density ρ of a graph as the total number of edges in a graph, divided by the total number of possible edges in the graph, given by the equation $\rho = \frac{|E|}{|V|(|V|-1)}$ for directed graphs and $\rho = \frac{2|E|}{|V|(|V|-1)}$ for undirected graphs. To vary the density of the generated graphs, we create a graph that is denser than our target parameter, ρ , and then

delete extraneous edges to meet the desired density. To limit the effect of this deletion on the graph's degree distribution, we select the edges to be deleted uniformly at random.

4.3 Synthetic Graphs

For each experiment on synthetic graphs, we vary the aforementioned parameters from §4.2, one at a time, leading to six sets of synthetic graphs, as shown in Table 2. Due to the interactions between inputs during graph generation, we do sometimes see significant changes in an unintended parameter (most notably in the graphs where the number of communities is varied), but to the best of our knowledge completely eradicating such interactions is impossible without breaking the parameters of the underlying DCSBM.

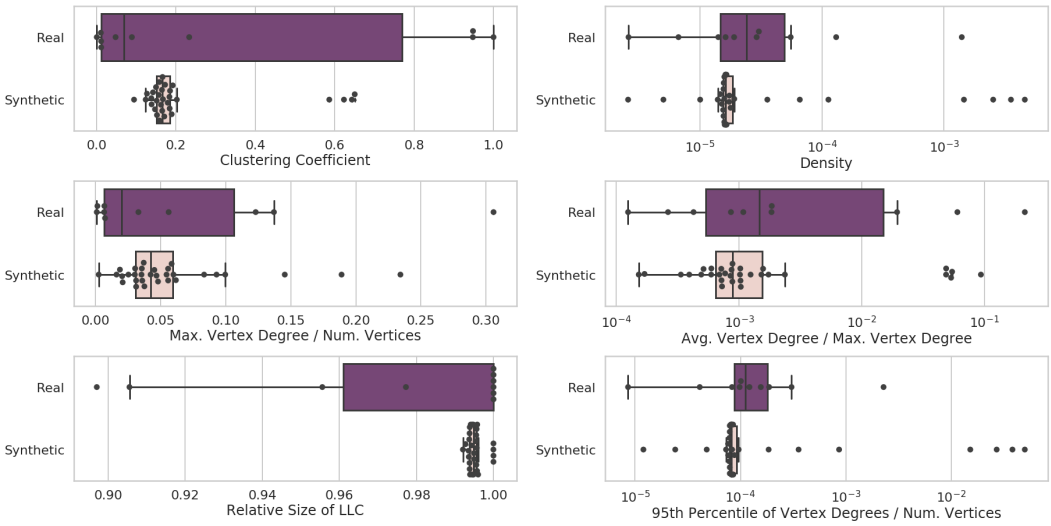


Fig. 5. Comparison of distributions of parameters of real-world graphs and our synthetically generated graphs. The synthetic graph parameters are clustered around the average parameter values for the real-world graphs, while still having enough of a spread to sweep over the range of the parameter values for the real-world graphs. Note the log scale on the x-axis for plots on the right.

4.3.1 Similarity to Real-World Graphs. To ensure that the results obtained from the synthetically generated graphs are applicable to real-world data, we compare our graphs to the selected web graphs. However, because we do not know the real community structure of the web graphs, we cannot compare parameters like C , σ , or s between the two sets of graphs. Additionally, many graph features depend on and scale with other features. As an example, the number of edges in a graph and the maximum vertex degree tend to increase as the number of vertices in the graph increases. Therefore, in order to compare our synthetic graphs to these web graphs, we heavily utilize ratios of parameters. As can be seen in Figure 5, our synthetic graphs are similar to the chosen web graphs with respect to the following parameters:

- Clustering coefficient
- Density (ρ) of the graph
- Ratio of maximum vertex degree d^{max} to number of vertices $|V|$
- Ratio of average vertex degree d^{avg} to maximum vertex degree d^{max}

Table 2. Parameters of Synthetically Generated Graphs

| ID | Parameter Varied | $ V $ | $ E $ | C | σ | s | d^{max} | ρ |
|-----|------------------|---------|----------|------|----------|------|-----------|-----------|
| S1 | $ V $ | 64496 | 273434 | 268 | 149.87 | 3.85 | 3595 | 6.573E-05 |
| S2 | $ V $ | 129533 | 597592 | 380 | 211.80 | 3.90 | 12903 | 3.562E-05 |
| S3 | $ V $ | 259804 | 1287506 | 537 | 287.99 | 3.84 | 9608 | 1.908E-05 |
| S4 | $ V $ | 522188 | 2732476 | 760 | 411.01 | 3.85 | 31255 | 1.002E-05 |
| S5 | $ V $ | 1039265 | 5409988 | 1075 | 588.38 | 3.87 | 21210 | 5.009E-06 |
| S6 | $ V $ | 2083515 | 11162085 | 1521 | 833.78 | 3.87 | 63287 | 2.571E-06 |
| S7 | C | 301090 | 1481756 | 128 | 1493.26 | 3.91 | 25109 | 1.635E-05 |
| S8 | C | 302724 | 1449717 | 256 | 681.76 | 3.75 | 18684 | 1.582E-05 |
| S9 | C | 302645 | 1509053 | 512 | 368.37 | 3.89 | 16860 | 1.648E-05 |
| S10 | C | 304063 | 1471727 | 1024 | 188.92 | 3.94 | 9472 | 1.592E-05 |
| S11 | C | 307653 | 1495872 | 2048 | 92.97 | 3.92 | 6403 | 1.580E-05 |
| S12 | σ | 308449 | 1480647 | 582 | 185.90 | 3.27 | 10878 | 1.556E-05 |
| S13 | σ | 304913 | 1469760 | 582 | 272.72 | 3.63 | 9491 | 1.581E-05 |
| S14 | σ | 303859 | 1524083 | 582 | 317.58 | 3.85 | 11397 | 1.651E-05 |
| S15 | σ | 302268 | 1475727 | 582 | 362.42 | 4.15 | 14143 | 1.615E-05 |
| S16 | σ | 300340 | 1563498 | 582 | 414.17 | 4.49 | 17541 | 1.733E-05 |
| S17 | s | 306600 | 1419360 | 582 | 326.65 | 1.32 | 10896 | 1.510E-05 |
| S18 | s | 302745 | 1425898 | 582 | 340.58 | 2.67 | 10862 | 1.556E-05 |
| S19 | s | 302686 | 1416219 | 582 | 325.42 | 3.89 | 9120 | 1.546E-05 |
| S20 | s | 302795 | 1488953 | 582 | 317.61 | 5.13 | 12799 | 1.624E-05 |
| S21 | s | 302140 | 1480226 | 582 | 336.49 | 6.58 | 13644 | 1.621E-05 |
| S22 | d^{max} | 300709 | 1262653 | 582 | 326.01 | 3.90 | 4841 | 1.396E-05 |
| S23 | d^{max} | 301394 | 1330587 | 582 | 319.70 | 3.86 | 5634 | 1.465E-05 |
| S24 | d^{max} | 302935 | 1434083 | 582 | 318.55 | 3.87 | 7637 | 1.563E-05 |
| S25 | d^{max} | 306094 | 1629938 | 582 | 313.75 | 3.85 | 14684 | 1.740E-05 |
| S26 | d^{max} | 305399 | 1658958 | 582 | 348.05 | 4.03 | 71531 | 1.779E-05 |
| S27 | ρ | 109575 | 55160457 | 336 | 182.55 | 3.88 | 20709 | 4.594E-03 |
| S28 | ρ | 108019 | 41269632 | 336 | 184.69 | 3.91 | 15702 | 3.537E-03 |
| S29 | ρ | 105044 | 27906832 | 336 | 181.69 | 3.91 | 9762 | 2.529E-03 |
| S30 | ρ | 99138 | 14312960 | 336 | 174.69 | 3.92 | 5407 | 1.456E-03 |
| S31 | ρ | 55548 | 347952 | 336 | 112.57 | 4.03 | 134 | 1.128E-04 |

- Relative size of largest connected component (as defined by $\frac{|V^C|}{|V|}$, where $|V^C|$ is the number of vertices in the largest connected component (LLC))
- Ratio of 95th percentile of vertex degrees d^{95} to number of vertices $|V|$

For each parameter, the values of the synthetic graphs are clustered around the average value for the real-world graphs, showing that our graphs are similar to the average web graph. The spread of the parameter values for the real-world graphs in Figure 5 shows that we have enough variation to sweep over the range of values that each parameter takes in real-world graphs.

4.4 Hardware and Software Infrastructure

We performed all of our experimental runs on the Intel®DevCloud, using computational nodes with 192 GB of memory and two Intel®Xeon®Gold 6128 processors, each supporting 12 concurrent threads. We make use of graph-tool’s built-in OpenMP-based parallelization of SBP and implement the sampling approach code in serial Python using the NumPy library [32, 47].

5 EXPERIMENTS ON SYNTHETIC GRAPHS

In this section, we describe a set of experiments performed on the synthetic graphs in Table 2. For every graph, we run our sampling approach using each of the five sampling algorithms from §3.3 at the 50%, 30% and 10% sample sizes. To provide a baseline for comparison, we run the SBP algorithm on the full graph without sampling. Additionally, we run our sampling approach *without* thresholding on graphs S1 to S6 using the ES, RNN, UR and FF sampling algorithms. Both the baseline and the SBP step of our sampling approach are implemented via the same OpenMP-parallelized call to the graph-tool [36] library.

Due to the stochastic nature of SBP, the algorithm can get stuck in a local minimum, leading to sub-optimal results on some runs and a large variance in the quality of community detection results. To reduce this variance, it is common practice to execute the algorithm multiple times independently, and select the best result [8]. We incorporate this technique into our approach by performing 5 runs for each experiment, where each run consists of 2 independent executions of SBP.

We evaluate two aspects of our approach: the speedup achieved and the quality of results. We evaluate the speedup by comparing the execution times of the runs with our sampling approach to the baseline runs. Similar to the Graph Challenge [17], we evaluate the quality of results by matching the communities obtained during the selected run to the true community memberships for each vertex using the Hungarian algorithm, and then calculating the F1 score, where

$$\text{F1 Score} = \frac{2 \times \text{Pairwise Precision} \times \text{Pairwise Recall}}{\text{Pairwise Precision} + \text{Pairwise Recall}}. \quad (6)$$

5.1 Thresholded Sampling Results

Here we evaluate our thresholded sampling approach on graphs S1-S6 and compare it to our sampling approach without thresholding. The MD sampling algorithm is excluded from these experiments since thresholding has no effect on it. Figure 6 compares the speedups and F1 scores obtained with and without *thresholded* sampling at the 50% and 30% sample sizes. At both sample sizes, thresholding leads to higher average F1 scores and lower variation in F1 scores, showing that it is highly likely to improve the quality of our sampling approach. However, this approach also leads to a drop in average speedup from 2.7× to 2.0× at the 50% sample size (though at the 30% sample size, average speedup remains roughly unchanged). At the 10% sample size, the difference between runs with and without thresholding is not significant because a 10% sample size is generally not large enough to capture all of the necessary structural information from the graph.

5.2 Result Summary

Across 31 graphs, we evaluate the performance of all five of our thresholded sampling algorithms. The results, summarized in Figure 7, show that MD sampling leads to the highest F1 scores on average. ES and RNN sampling achieve slightly lower F1 scores on average and have higher variation, but are still capable of reaching and even surpassing the F1 scores achieved by MD. FF and UR sampling perform the worst, with the lowest average F1 scores and the highest variability,

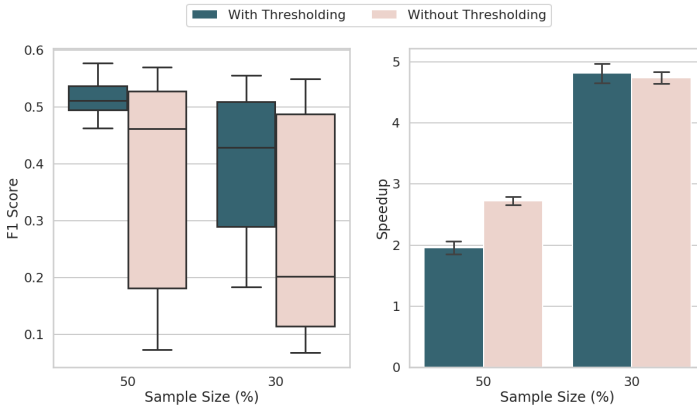


Fig. 6. Comparison of F1 scores (left) and average speedups compared to performing community detection without sampling (right) obtained with and without thresholding at the 50% and 30% sample sizes on graphs S1-S6. Results combine data from the uniform random, random node neighbor, forest fire, and expansion snowball sampling algorithms.

due to the presence of island vertices in the sampled graph. Overall, with the exception of FF, the topology-guided sampling algorithms lead to higher F1 scores.

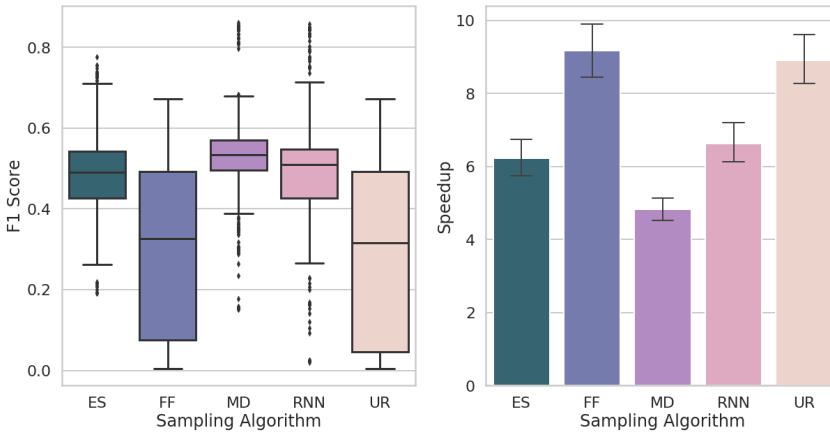


Fig. 7. Comparison of F1 scores (left) and average speedups compared to performing community detection without sampling (right) obtained using each of the five sampling algorithms, across all 31 synthetic graphs. Data includes the 10%, 30% and 50% sample sizes.

In terms of the speedup gained over community detection without sampling, however, MD sampling lags behind the other sampling algorithms. ES sampling, while relatively fast on smaller graphs, suffers from scalability issues at larger sample sizes; so much so that at the 50% sample size, it leads to slowdowns on graphs S4-S6 ($|V| \geq 522188$). FF and UR sampling, the worst performers in terms of accuracy, provide the highest speedups on average.

In light of the above results and for the sake of brevity, we only show results with the MD algorithm for the remainder of this section. On average, the thresholded MD algorithm delivers the

best F1 score while still achieving a significant average speedup of 4.8×. For results from all of our experiments conducted on synthetic graphs, refer to Appendix A.

5.3 Results for Individual Experiments

We conclude our analysis of the results obtained on synthetic graphs by identifying trends in the comparative quality of returned communities and speedups gained using our thresholded-sampling approach for each experiment.

5.3.1 Trends in Result Quality. First, we identify trends with respect to the quality of community detection results obtained. Though we only show the trends obtained with MD sampling, we find that they are closely replicated by the other sampling algorithms. The results discussed here are relative to the baseline SBP (i.e., 100% sample size). When the sampling approach achieves “good” F1 scores, the F1 scores achieved with sampling are comparable to those achieved by the baseline SBP. When the sampling approach leads to “poor” F1 scores, they are considerably lower than those achieved by the baseline.

Empirically, the scale of the graph (i.e., number of vertices) does not affect the quality of results obtained via sampling (see top graph in Figure 8). Although sampling leads to relatively poor F1 scores on graphs S3 (260k vertices) and S4 (522k vertices), it does achieve good results on the smaller graphs S1 and S2 and on the larger graphs S5 and S6. Overall, the F1 scores achieved with and without sampling increase with the size of the graph. One factor that contributes to this is the sublinear increase in the number of communities with respect to $|V|$, as demonstrated in our own experiments in Figure 8 (middle), where F1 scores are higher in graphs with fewer communities.

In most of the remaining experiments, including those that varied the number of communities C (graphs S7-S11, Figure 8, middle), the strength of the communities s (graphs S17-S21, Figure 8, bottom), the maximum vertex degree d^{max} (S22-S26, Figure 9, top), and density ρ (graphs S27-S31, Figure 9, middle), our approach works best when the aforementioned parameters are low. So much so that, on graphs S7-S9 ($C \leq 512$), S17-S18 ($s \leq 2.67$), S22-S23 ($d^{max} \leq 5634$), and S27 ($\rho = 0.0001$), we achieve *higher* F1 scores with our sampling approach than the baseline. In S17 and S27, F1 scores with sampling at the 50% sample size are over twice as high as F1 scores without sampling.

On the other hand, the experiments with community size variation σ (S12-S16, Figure 9, bottom) show the reverse trend, and we are unable to achieve higher F1 scores with sampling than the baseline, with the possible exception of graph S14, where the average F1 score with sampling is very slightly higher at the 50% sample size.

5.3.2 Trends in Speedup. Next, we identify the trends in speedup with respect to the parameters modified in each experiment. For the majority of the studied graph parameters, including graph size $|V|$ (graphs S1-S6, Figure 10), number of communities C (graphs S7-S11, Figure 10), the standard deviation in community size σ (graphs S12-S16, Figure 10), and the strength of community structure s (graphs S17-S21, Figure 11), our results indicate that varying the parameter does not affect speedup by a significant amount. The 10% sample size is the exception, where speedup generally increases as $|V|$ and s increase.

On the other hand, maximum vertex degree d^{max} (graphs S22-26, Figure 11) and density ρ (graphs S27-S31, Figure 11) do affect speedup. As d^{max} increases, the percentage of edges present in the sampled graph increases, causing the SBP step of our sampling approach to take longer, and the average speedup obtained to decrease.

Experiments with ρ show a more complicated pattern; speedup at the 10% sample size increases as density increases, but at the 50% and 30% sample sizes, speedup is highest at the lowest ρ (graph S27), after which it drops drastically and then gradually increases as ρ increases. These results can be explained by a combination of two factors. First, SBP is faster at lower densities because

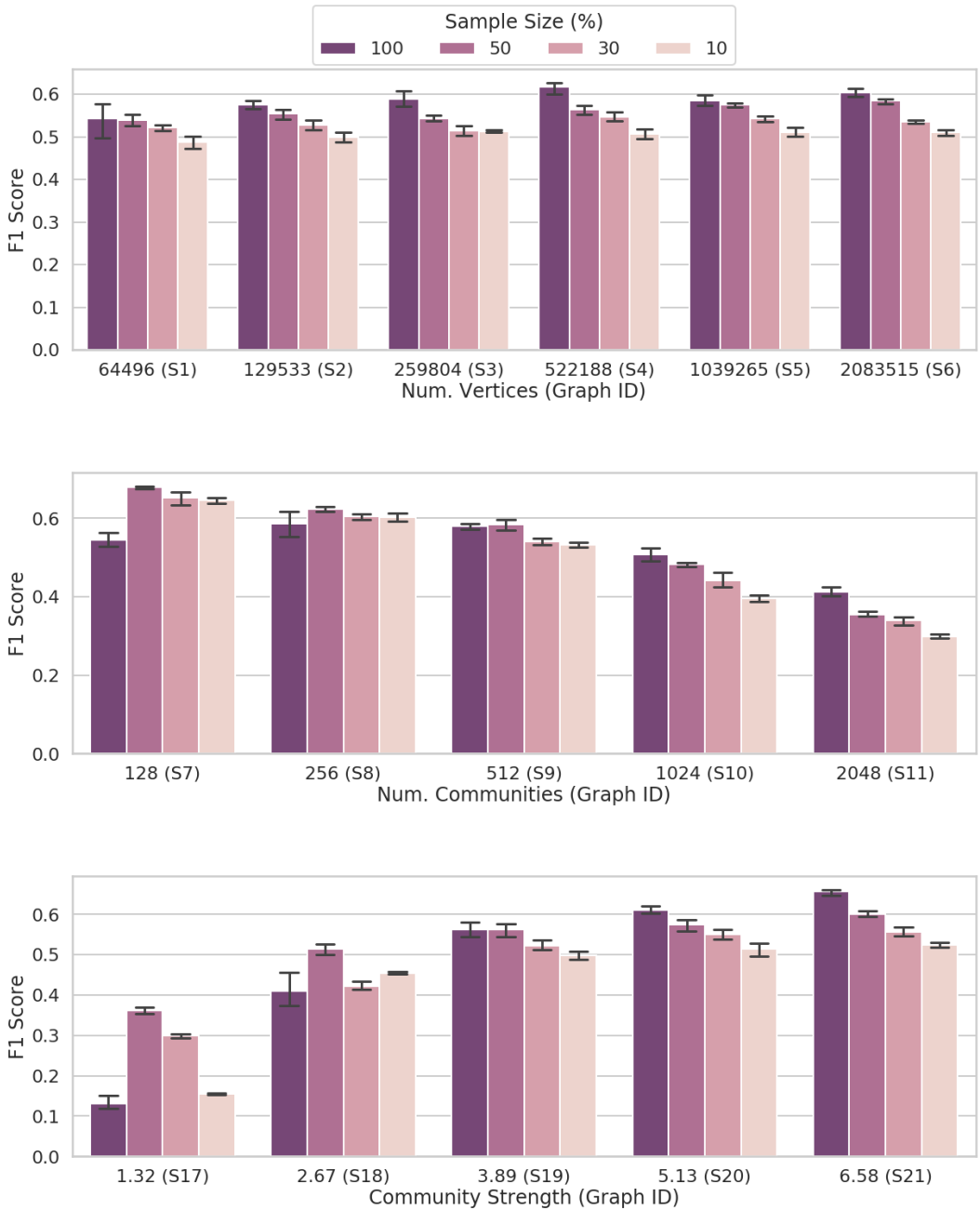


Fig. 8. Comparison of F1 scores for three different experiments using maximum degree sampling. The 100% sample size represents the baseline of running stochastic block partitioning without sampling. Top: scaling experiments (graphs S1-S6). Middle: number of communities experiments (graphs S7-S11). Bottom: strength of community structure experiments (graphs S17-S21).

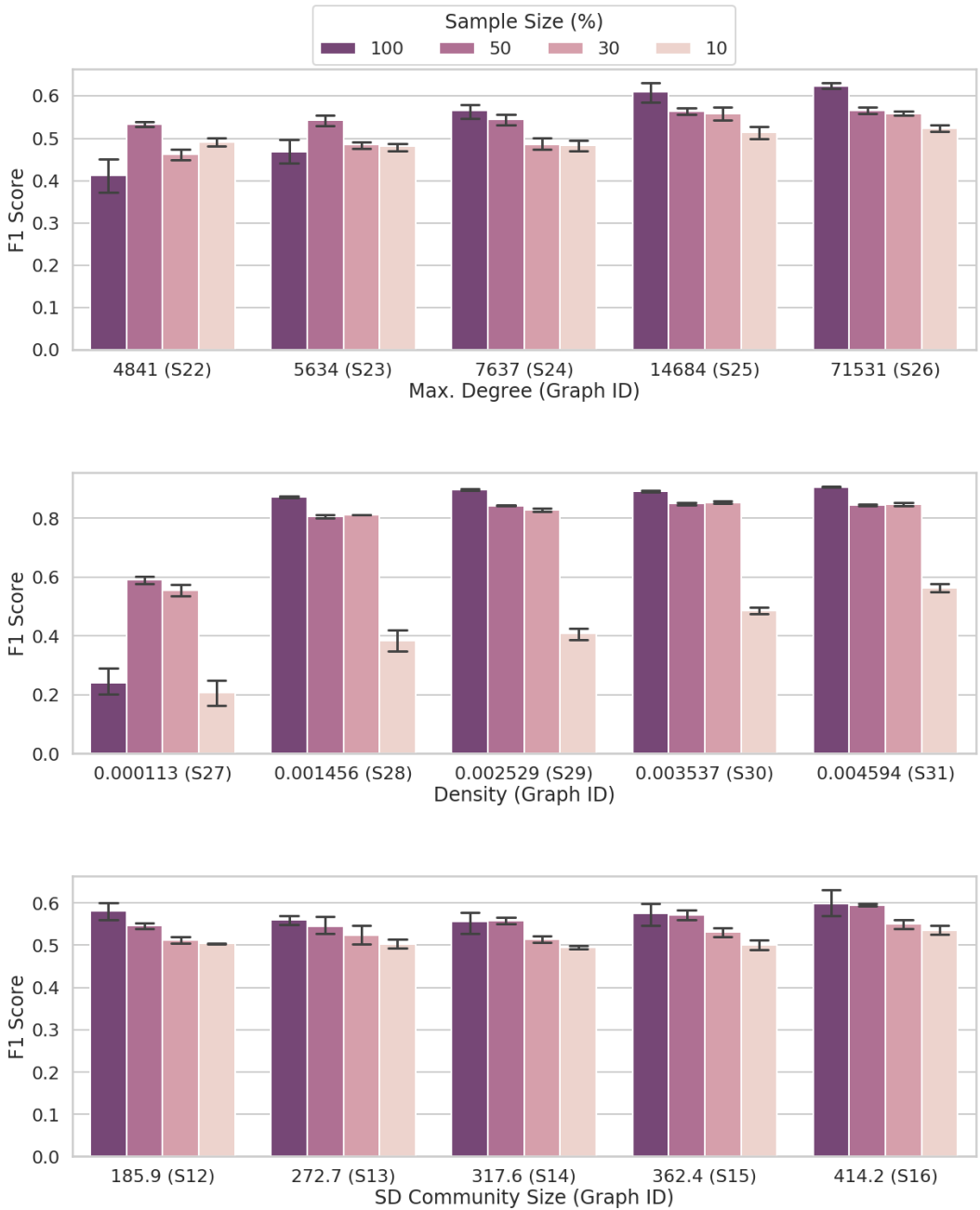


Fig. 9. Comparison of F1 scores for three different experiments using maximum degree sampling. The 100% sample size represents the baseline of running stochastic block partitioning without sampling. Top: maximum vertex degree experiments (graphs S22-S26). Middle: density experiments (graphs S27-S31). Bottom: variation in community size experiments (graphs S12-S16).

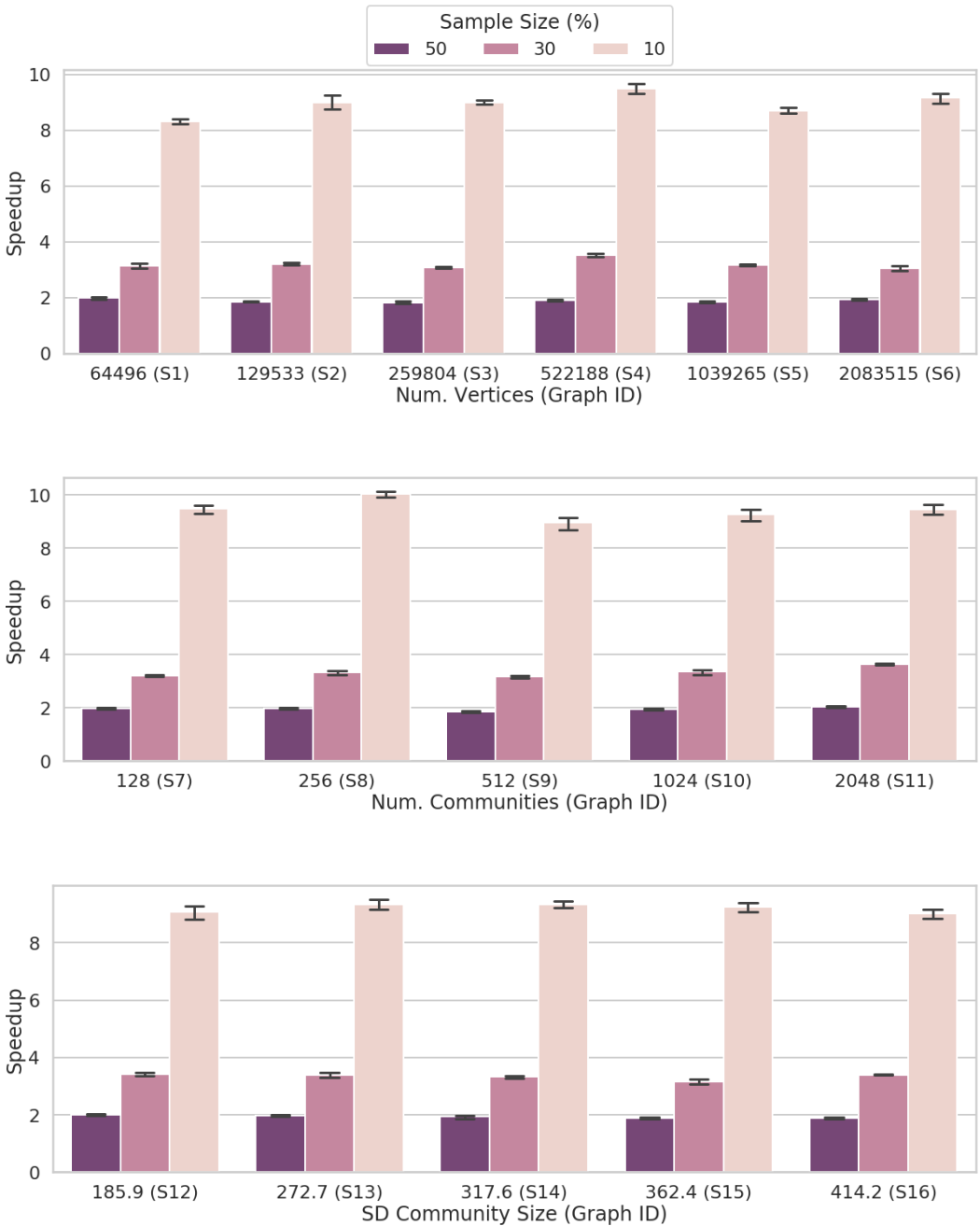


Fig. 10. Comparison of speedup obtained over the baseline (stochastic block partitioning without sampling) for three different experiments using maximum degree sampling. Top: scaling experiments (graphs S1-S6). Middle: number of communities experiments (graphs S7-S11). Bottom: variation in community size experiments (graphs S12-S16).

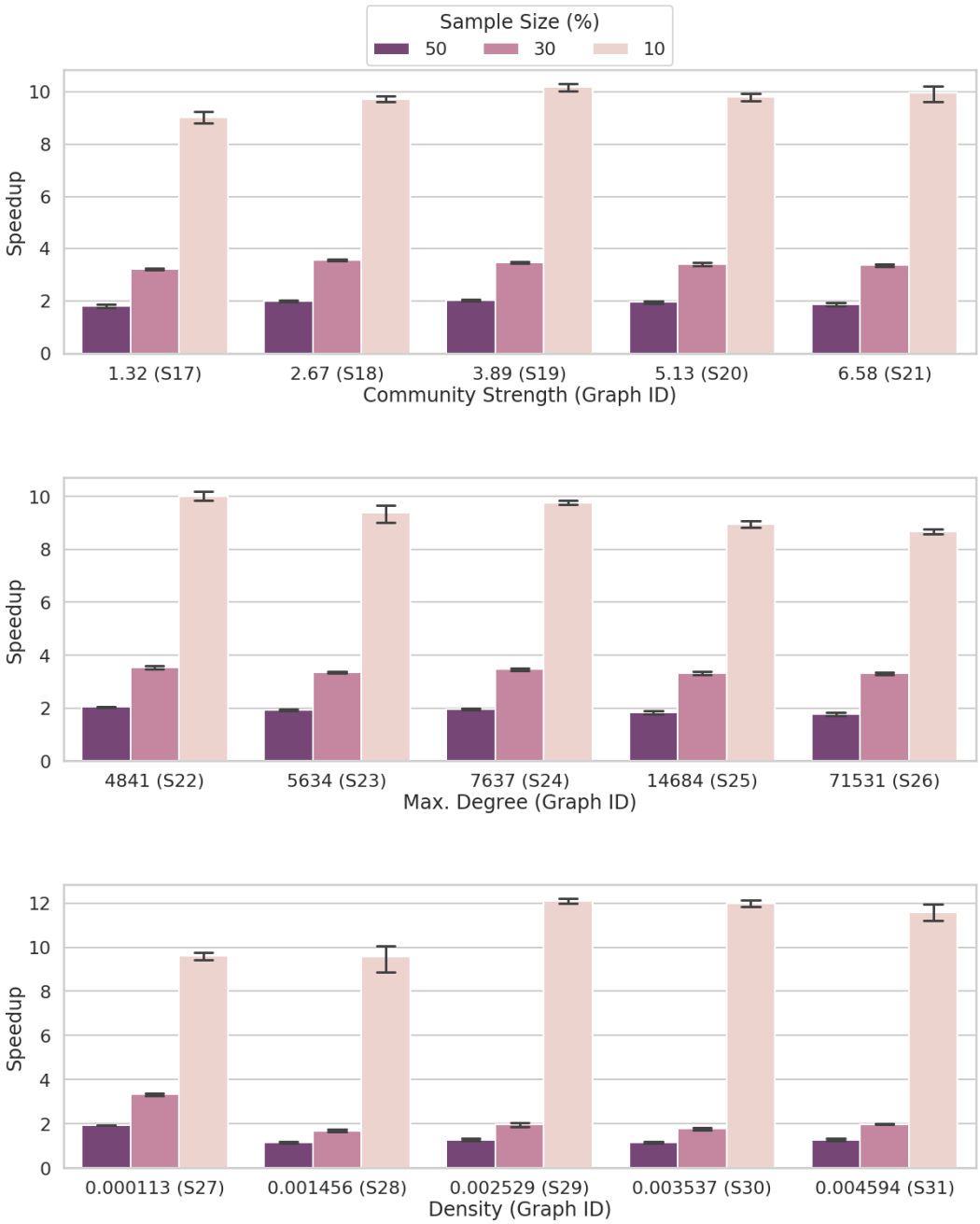


Fig. 11. Comparison of speedup obtained over the baseline (stochastic block partitioning without sampling) for three different experiments using maximum degree sampling. Top: strength of community structure experiments (graphs S17-S21). Middle: maximum vertex degree experiments (graphs S22-S26). Bottom: density experiments (graphs S27-S31).

the algorithm has to process fewer edges. This means that at lower densities, and especially when the low density is combined with a low sample size, the amount of time taken to propagate the community memberships from the sampled graph to the remaining vertices, and to finetune the results, becomes more significant. The second factor is that, similarly to the d^{max} experiments, the percentage of edges present in the sampled graph increases as the graph density increases, leading to lower speedups at higher sample sizes.

5.4 Discussion

One would intuitively expect that an approach based on data reduction would work best for simpler graphs, where the community structure is more obvious. For our experiments, this would translate to better F1 scores in comparison to the baseline when the baseline F1 scores are high. However, for many experiments, including s , d^{max} , and ρ , sampling performs much better when the graph's communities are harder to accurately detect. Additionally, although σ does not have a strong effect on baseline F1 scores, our sampling approach performs better comparatively when σ is high, despite the fact that the community sizes are more uneven, making it harder to perform community detection on those graphs.

We postulate that the explanation for this phenomenon lies in the relative amount of information captured via sampling. Intuitively, graphs that present a harder community detection problem would contain fewer vertices that provide useful structural information. For example, when the graph is too sparse, several vertices could have unclear community memberships because they're connected to only 1 other vertex. Similarly, when the community structure is not strong, vertices may be equally strongly connected to several communities. In such cases, a good sampling algorithm could narrow the search space for the MCMC process down to just the vertices that provide useful structural information, leading to good community detection results.

Additionally, narrowing down the search space could make it easier for the SBP algorithm to find the globally optimal solution, provided that the search space still contains enough structural information. This could explain how sampling sometimes leads to better community detection results than the baseline; the baseline algorithm simply gets stuck in a locally optimal solution.

Another anomaly in our results is that FF sampling leads to relatively poor F1 scores despite being a topology-guided sampling method. We believe that this is because the algorithm "burns" too many vertices by marking them as visited but not selected. Given the sparsity of our set of graphs, the fact that they are directed, and the fact that the algorithm is not allowed to revisit vertices, it becomes easy for the algorithm to get stuck, at which point sampling is restarted from a new vertex. Each restart is then progressively more likely to get stuck, leading to many small disconnected components and island vertices, as seen in Figure 4. The choice of hyperparameter p may reduce this effect, but the optimal value of p is unknown and likely to be specific to each graph. Searching for the optimal sampling algorithm parameters is outside the scope of this work, and unless a recommendation can be made a priori, we argue that this failure mode is significant enough to focus on other sampling algorithms for our set of experiments.

Several avenues for future work present themselves based on these results. One would be a factorial experiment design to identify more complex performance patterns that exist due to interactions between graph parameters. Another is developing parallel or even distributed versions of the sampling algorithms, which could lead to further speedup gains, especially on large graphs. Lastly, a deep dive into our approach on the graphs where sampling improved result quality could lead to a more concrete explanation of the aforementioned phenomenon, and maybe even provide a theoretical intuition into how to achieve the same effect on other graphs.

6 EXPERIMENTS ON REAL-WORLD GRAPHS

In this section, we describe the experiments performed on the set of real-world web graphs from Table 1.

6.1 Evaluation Metric

Performing community detection on real-world graphs often presents the problem of *not* knowing what the true community memberships are. This makes it difficult to evaluate the quality of community detection results, since straightforward metrics such as accuracy and F1 score cannot be calculated without this knowledge a priori.

A popular way of evaluating community detection results in such situations is calculating the modularity of the resulting community structure. Modularity measures how strongly vertices within communities are connected, as compared to a random graph, making it an intuitive choice for evaluating community detection. However, it has been shown that high modularity values do *not* necessarily correspond to the most semantically accurate community assignments [5]. Additionally, we argue that modularity ignores several important factors, such as the number of communities obtained and the degree distributions within these communities, factors that are important in describing the community structure of a graph.

To overcome these weaknesses, we devise an alternative evaluation metric based on the minimum description length H of the DCSBM. By basing our evaluation on H , our metric takes into account both the number of communities obtained and the difference in degree distribution between communities via log-likelihood calculations (see §2.3). Furthermore, the goal of SBP is to minimize H . As such, comparing the values of H obtained with and without sampling is a natural way to evaluate distinct community detection approaches that use the SBP algorithm.

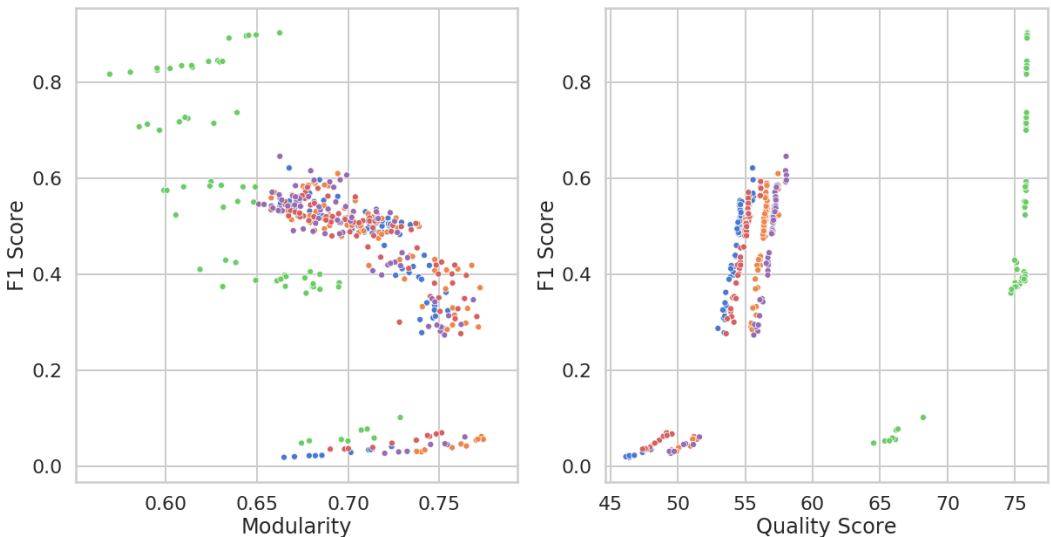


Fig. 12. Comparison of the relationships between F1 Score and Modularity (left) and F1 Score and Quality Score (right). To reduce clutter, we only show results for five randomly-selected synthetic graphs that are colored by graph ID. Each point represents a single community detection run (after simulating multiple MCMC chains), using either the baseline algorithm or our sampling approach with thresholding. The data includes 10%, 30%, and 50% sample sizes, and all five sampling algorithms.

where H^{max} is the maximum possible value of H for a given graph (when every vertex is considered to be a separate community), and H is the minimum description length obtained via performing SBP on the same graph.

Our metric, the *Quality Score* QS , is defined as the amount of the blockmodel minimum description length that has been compressed through performing community detection. QS is given by the following equation:

$$QS = \frac{H^{max} - H}{H^{max}}, \quad (7)$$

To evaluate QS and modularity, we collect both metrics for our synthetic experimental runs, as articulated in §5, and compare them to the obtained F1 scores. As Figure 12 shows, modularity does *not* correspond well to the F1 scores obtained. In fact, for roughly half of our data points, modularity has an inverse relationship with F1 score. This is consistent with the findings in [52], which show that modularity has an inverse relationship with several measures of community quality. On the other hand, QS has a much more direct relationship with F1 score.

6.2 Experiments

To evaluate our approach on real-world graphs, we adopt a similar approach to the one described in §5 but with fewer parameters. For every graph in Table 1, we run our sampling approach using the three best-performing sampling algorithms from §5 — MD, RNN and ES — but with thresholding. We only run these algorithms at the 30% sample size as a compromise between speedup and quality of community detection. To provide a baseline for comparison, we also run the SBP algorithm on each full graph without sampling.

We evaluate two aspects of our approach; the speedup gained and the quality of results. We evaluate the speedup by comparing the execution times of the runs with our sampling approach to the baseline runs and the quality of results using the *Quality Score* metric described above. For the results on all experiments performed, refer to Appendix B.

6.3 Results on Web Graphs

Similar to the results on the synthetic graphs, we find that MD sampling generally produces the best results on real-world graphs. As Figure 13 shows, the quality of results using our sampling approach is very similar to the baseline. In fact, for all 10 real-world graphs, our sampling approach achieves a QS within just 0.05 of the baseline.

The most intriguing result occurs on graph R10. It is the only graph on which there is a large difference in QS between the tested sampling algorithms; it is also the only graph on which MD sampling leads to a poor QS . However, as shown in Figure 14, ES sampling achieves good QS results on the same graph. This outlier result can be explained by the composition of the communities within the R10 graph. Because MD sampling only samples the vertices with the highest degree, communities comprised of only low-degree vertices will *not* be present in the sample, and thus, cannot be identified using our sampling approach. Upon examination of the communities obtained without sampling on R10, we find that only 37.5% of them contain vertices with a high-enough degree to be selected by the MD algorithm at the 30% sample size. The ES sampling algorithm, which prioritizes exploration of the graph, is unaffected by this phenomenon. The RNN algorithm, while performing better than MD, is also prone to undersampling such communities when the number of communities with high-degree vertices is large.

With MD sampling at the 30% sample size, we achieve an average speedup of 2.36× across the web graphs R1-R10. As Figure 15 shows, there is a relatively wide range of obtained speedups from only 1.16× on R8 to 3.84× on the much denser R10. RNN and ES sampling regularly result in higher

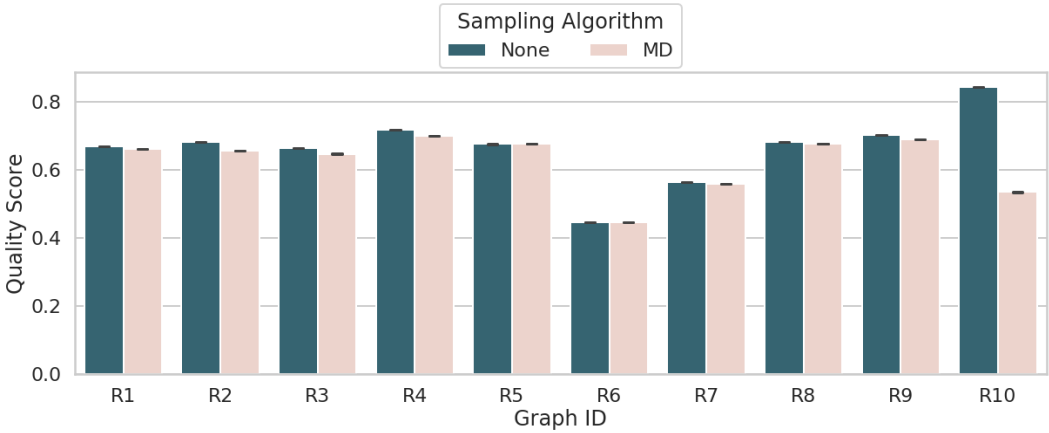


Fig. 13. Comparison of the Quality Score achieved on 10 web graphs with and without our sampling approach (higher is better). The maximum degree sampling algorithm (MD) ran with a 30% sample size.

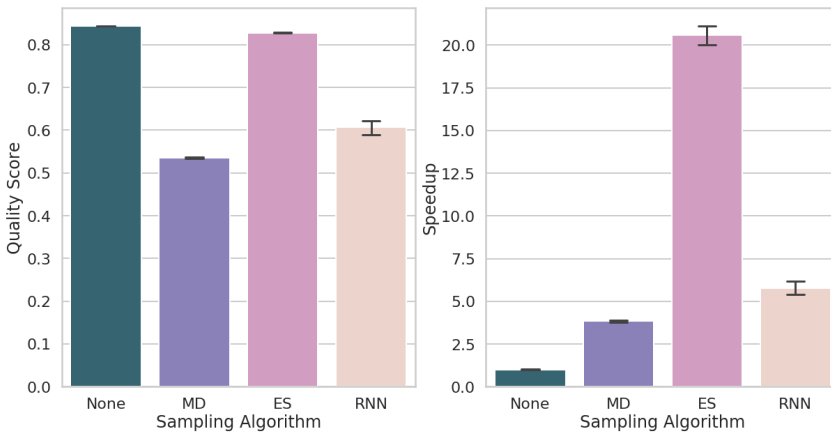


Fig. 14. Comparison of the Quality Score (left, higher is better) and average speedups (right) achieved on graph R10 (web-uk-2005) using the baseline, maximum degree (MD), expansion snowball (ES), and random node neighbor (RNN) sampling algorithms at the 30% sample size.

speedups, most notably with ES achieving a speedup of over 20× on R10 at the same sample size. This is largely due to ES sampling producing much sparser sampled graphs, which results in more rapid blockmodel inference.

6.4 Discussion

The outlier graph R10 shows that the choice of sampling algorithm depends on the structure of the graph. While our synthetic graphs do not capture the behavior of R10, our own experiments on the Graph Challenge [17] graphs showed a similar pattern to R10, where ES sampling produces better quality results than the other sampling algorithms, including RNN. This raises the question of whether or not other graph parameters exist that similarly affect the choice of sampling algorithm.

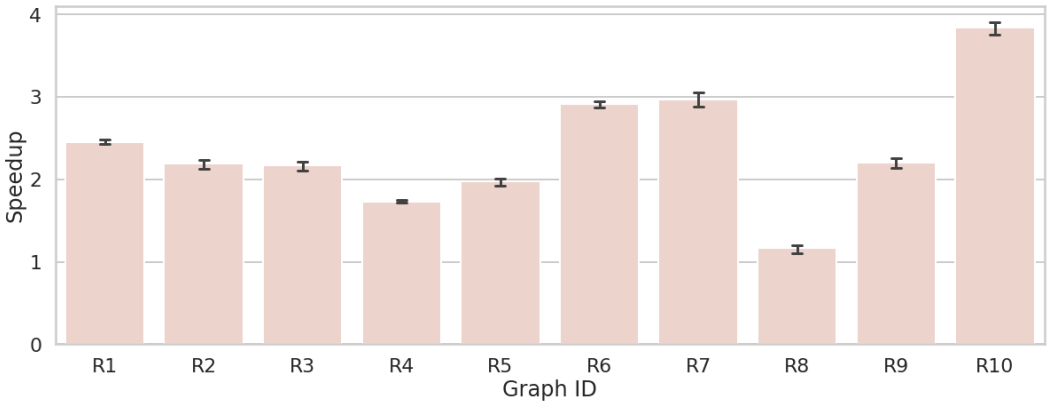


Fig. 15. Comparison of the speedups obtained on 10 web graphs with our sampling approach over the baseline, using the maximum degree (MD) sampling algorithm at the 30% sample size.

On the whole, however, the results in this section provide strong evidence that our sampling approach works well on real-world graphs. This is despite the fact that we only considered a 30% sample size in these experiments; our preliminary results [49] suggest that generally a 35%-45% sample size is needed to achieve near-optimal result quality.

For future work, we envision extended testing of the generalizability of our approach by applying it to several categories of real-world graphs, including protein interaction networks and social network graphs. Additionally, we would like to see our approach applied to overlapping community detection, which is a more accurate representation of the real-world scenario, albeit more computationally expensive.

7 CONCLUSION

In this manuscript, we present a four-step sampling-based approach to accelerate community detection as well as a thresholding technique for improving the efficacy of sampling for this purpose. We generate graphs with community structure based on the degree-corrected stochastic blockmodel (DCSBM), and we perform a series of experiments to determine the effects of various graph parameters on the quality of results and speedup obtained using our approach across different sampling algorithms and different sample sizes. Additionally, we provide empirical evidence that thresholding improves the quality of community detection results with sampling and that this quality of results is also preserved in real-world graphs.

Our sampling-based approach is flexible; the choice of sampling algorithm (see Figure 7) and sample size (see Figure 1) allows the user to make a trade-off between speedup and quality of result. This is exemplified by our achieving a speedup of up to 15 \times without sacrificing result quality or by improving result quality (i.e., F1 score) by over 150% at a speedup of around 2 \times . If some degradation in result quality is not an issue, we can achieve speedups as high as 45 \times (see Appendix A). Moreover, the experimental results show that our topology-guided sampling approach improves the result quality on graphs with weak community structure, as characterized by low community strength, maximum vertex degree, and density.

ACKNOWLEDGMENTS

Computing resources supporting this work were provided by Intel®Development Tools through the Intel®DevCloud.

We thank Atharva Gondhalekar and Sajal Dash for their insightful comments and discussion.

REFERENCES

- [1] Maciej Besta, Simon Weber, Lukas Gianinazzi, Robert Gerstenberger, Andrey Ivanov, Yishai Oltchik, and Torsten Hoefler. 2019. Slim graph. In *Proceedings of the International Conference for High Performance Computing, Networking, Storage and Analysis*. ACM, New York, NY, USA, 1–25. <https://doi.org/10.1145/3295500.3356182>
- [2] Vincent D Blondel, Jean-Loup Guillaume, Renaud Lambiotte, and Etienne Lefebvre. 2008. Fast unfolding of communities in large networks. *Journal of Statistical Mechanics: Theory and Experiment* 2008, 10 (10 2008), P10008. <https://doi.org/10.1088/1742-5468/2008/10/P10008>
- [3] Anne Condon and Richard M. Karp. 2001. Algorithms for graph partitioning on the planted partition model. *Random Structures and Algorithms* 18, 2 (3 2001), 116–140. [https://doi.org/10.1002/1098-2418\(200103\)18:2<116::AID-RSA1001>3.0.CO;2-2](https://doi.org/10.1002/1098-2418(200103)18:2<116::AID-RSA1001>3.0.CO;2-2)
- [4] Paul Erdős and Alfréd Rényi. 1984. The evolution of random graphs. *Trans. Amer. Math. Soc.* 286 (1984), 257–257. <https://doi.org/10.1090/S0002-9947-1984-0756039-5>
- [5] Santo Fortunato. 2010. Community detection in graphs. *Physics Reports* 486, 3-5 (2 2010), 75–174. <https://doi.org/10.1016/J.PHYSREP.2009.11.002>
- [6] S. Fortunato and M. Barthelemy. 2007. Resolution limit in community detection. *Proceedings of the National Academy of Sciences* 104, 1 (1 2007), 36–41. <https://doi.org/10.1073/pnas.0605965104>
- [7] Ruohan Gao, Huanle Xu, Pili Hu, and Wing Cheong Lau. 2016. Accelerating graph mining algorithms via uniform random edge sampling. In *2016 IEEE International Conference on Communications (ICC)*. IEEE, 1–6. <https://doi.org/10.1109/ICC.2016.7511156>
- [8] Andrew Gelman, John B. Carlin, Hal S. Stern, David B. Dunson, Aki Vehtari, and Donald B. Rubin. 2013. *Bayesian Data Analysis*. Chapman and Hall/CRC. <https://doi.org/10.1201/b16018>
- [9] Sayan Ghosh, Mahantesh Halappanavar, Antonino Tumeo, and Ananth Kalyanarainan. 2019. Scaling and Quality of Modularity Optimization Methods for Graph Clustering. In *2019 IEEE High Performance Extreme Computing Conference (HPEC)*. IEEE, 1–6. <https://doi.org/10.1109/HPEC.2019.8916299>
- [10] Sayan Ghosh, Mahantesh Halappanavar, Antonino Tumeo, Ananth Kalyanaraman, and Assefaw H Gebremedhin. 2018. Scalable Distributed Memory Community Detection Using Vite. In *2018 IEEE High Performance Extreme Computing Conference (HPEC'18)*. Waltham, MA. <https://doi.org/10.1109/HPEC.2018.8547534>
- [11] Sayan Ghosh, Mahantesh Halappanavar, Antonino Tumeo, Ananth Kalyanaraman, and Assefaw H. Gebremedhin. 2018. Scalable Distributed Memory Community Detection Using Vite. In *2018 IEEE High Performance extreme Computing Conference (HPEC)*. IEEE, 1–7. <https://doi.org/10.1109/HPEC.2018.8547534>
- [12] Sayan Ghosh, Mahantesh Halappanavar, Antonino Tumeo, Ananth Kalyanaraman, Hao Lu, Daniel Chavarria-Miranda, Arif Khan, and Assefaw Gebremedhin. 2018. Distributed Louvain Algorithm for Graph Community Detection. In *2018 IEEE International Parallel and Distributed Processing Symposium (IPDPS)*. IEEE, 885–895. <https://doi.org/10.1109/IPDPS.2018.00098>
- [13] Mahantesh Halappanavar, Hao Lu, Ananth Kalyanaraman, and Antonino Tumeo. 2017. Scalable static and dynamic community detection using Grappolo. In *2017 IEEE High Performance Extreme Computing Conference (HPEC)*. IEEE, 1–6. <https://doi.org/10.1109/HPEC.2017.8091047>
- [14] W. K. Hastings. 1970. Monte Carlo sampling methods using Markov chains and their applications. *Biometrika* 57, 1 (4 1970), 97–109. <https://doi.org/10.1093/biomet/57.1.97>
- [15] Bernardo A. Huberman and Lada A. Adamic. 1999. Growth dynamics of the World-Wide Web. *Nature* 401, 6749 (9 1999), 131–131. <https://doi.org/10.1038/43604>
- [16] Yuting Jia, Qinqin Zhang, Weinan Zhang, and Xinbing Wang. 2019. CommunityGAN: Community Detection with Generative Adversarial Nets. In *Proceedings of the World Wide Web Conference (WWW '19)*. ACM Press, New York, New York, USA, 784–794. <https://doi.org/10.1145/3308558.3313564>
- [17] Edward Kao, Vijay Gadepally, Michael Hurley, Michael Jones, Jeremy Kepner, Sanjeev Mohindra, Paul Monticciolo, Albert Reuther, Siddharth Samsi, William Song, Diane Staheli, and Steven Smith. 2017. Streaming graph challenge: Stochastic block partition. In *2017 IEEE High Performance Extreme Computing Conference (HPEC)*. IEEE, 1–12. <https://doi.org/10.1109/HPEC.2017.8091040>
- [18] Edward K. Kao, Steven Thomas Smith, and Edoardo M. Airoldi. 2019. Hybrid Mixed-Membership Blockmodel for Inference on Realistic Network Interactions. *IEEE Transactions on Network Science and Engineering* 6, 3 (7 2019), 336–350. <https://doi.org/10.1109/TNSE.2018.2823324>
- [19] Brian Karrer and M. E. J. Newman. 2011. Stochastic blockmodels and community structure in networks. *Physical Review E* 83, 1 (1 2011), 016107. <https://doi.org/10.1103/PhysRevE.83.016107>
- [20] Balachander Krishnamurthy, Jia Wang, Balachander Krishnamurthy, and Jia Wang. 2000. On network-aware clustering of Web clients. In *ACM SIGCOMM Computer Communication Review*, Vol. 30. ACM, Stockholm, Sweden, 97–110.

- <https://doi.org/10.1145/347057.347412>
- [21] Andrea Lancichinetti, Santo Fortunato, and Filippo Radicchi. 2008. Benchmark graphs for testing community detection algorithms. *Physical Review E* 78, 4 (10 2008), 046110. <https://doi.org/10.1103/PhysRevE.78.046110>
 - [22] Jure Leskovec and Christos Faloutsos. 2006. Sampling from large graphs. In *Proceedings of the 12th ACM SIGKDD international conference on Knowledge discovery and data mining - KDD '06*. ACM Press, New York, New York, USA, 631. <https://doi.org/10.1145/1150402.1150479>
 - [23] Georgiy M. Levchuk and John Colonna-Romano. 2018. Optimizing collaborative computations for scalable distributed inference in large graphs. In *Signal Processing, Sensor/Information Fusion, and Target Recognition XXVII*, Ivan Kadar (Ed.), Vol. 10646. SPIE, 23. <https://doi.org/10.1117/12.2305872>
 - [24] Guo Li, Dafang Zhang, and Yanbiao Li. 2017. Packet Classification Using Community Detection. In *2017 IEEE International Symposium on Parallel and Distributed Processing with Applications and 2017 IEEE International Conference on Ubiquitous Computing and Communications (ISPA/IUCC)*. IEEE, Guangzhou, China, 94–100. <https://doi.org/10.1109/ISPA/IUCC.2017.00023>
 - [25] Xu Liu, Jesun Sahariar Firoz, Marcin Zalewski, Mahantesh Halappanavar, Kevin J. Barker, Andrew Lumsdaine, and Assefaw H. Gebremedhin. 2019. Distributed Direction-Optimizing Label Propagation for Community Detection. In *2019 IEEE High Performance Extreme Computing Conference (HPEC)*. IEEE, 1–6. <https://doi.org/10.1109/HPEC.2019.8916215>
 - [26] Hao Lu, Mahantesh Halappanavar, and Ananth Kalyanaraman. 2015. Parallel heuristics for scalable community detection. *Parallel Comput.* 47 (8 2015), 19–37. <https://doi.org/10.1016/J.PARCO.2015.03.003>
 - [27] Arun S. Maiya and Tanya Y. Berger-Wolf. 2010. Sampling community structure. In *Proceedings of the 19th international conference on World wide web - WWW '10*. ACM Press, New York, New York, USA, 701. <https://doi.org/10.1145/1772690.1772762>
 - [28] Nikhil Mehta, Lawrence Carin Duke, and Piyush Rai. 2019. Stochastic Blockmodels meet Graph Neural Networks. In *Proceedings of the 36th International Conference on Machine Learning*. PMLR, Vienna, Austria, 4466–4474. <http://proceedings.mlr.press/v97/mehta19a.html>
 - [29] Peter Morales, Rajmonda Sulo Caceres, and Tina Eliassi-Rad. 2020. Deep Reinforcement Learning for Task-Driven Discovery of Incomplete Networks. In *Complex Networks and Their Applications VIII*, Vol. 881 SCI. Springer, 903–914. https://doi.org/10.1007/978-3-030-36687-2_75
 - [30] Md. Naim, Fredrik Manne, Mahantesh Halappanavar, and Antonino Tumeo. 2017. Community Detection on the GPU. In *2017 IEEE International Parallel and Distributed Processing Symposium (IPDPS)*. IEEE, 625–634. <https://doi.org/10.1109/IPDPS.2017.16>
 - [31] Andrew Y Ng, Michael I Jordan, and Yair Weiss. 2001. On spectral clustering: analysis and an algorithm. In *Proceedings of the 14th International Conference on Neural Information Processing Systems: Natural and Synthetic*. MIT Press, Vancouver, British Columbia, Canada, 849–856. <https://doi.org/10.5555/2980539.2980649>
 - [32] Travis E Oliphant. 2006. *Guide to NumPy*. Trelgol Publishing. <https://ftp.tw.freebsd.org/distfiles/numpybook.pdf>
 - [33] Tiago P. Peixoto. 2013. Hierarchical Block Structures and High-resolution Model Selection in Large Networks. (10 2013). <https://doi.org/10.1103/PhysRevX.4.011047>
 - [34] Tiago P. Peixoto. 2013. Parsimonious Module Inference in Large Networks. *Physical Review Letters* 110, 14 (4 2013), 148701. <https://doi.org/10.1103/PhysRevLett.110.148701>
 - [35] Tiago P. Peixoto. 2014. Efficient Monte Carlo and greedy heuristic for the inference of stochastic block models. *Physical Review E* 89, 1 (1 2014), 012804. <https://doi.org/10.1103/PhysRevE.89.012804>
 - [36] Tiago P. Peixoto. 2014. The graph-tool python library. *figshare* (2014). <https://doi.org/10.6084/m9.figshare.1164194>
 - [37] Tiago P. Peixoto. 2017. Nonparametric Bayesian inference of the microcanonical stochastic block model. *Physical Review E* 95, 1 (1 2017), 012317. <https://doi.org/10.1103/PhysRevE.95.012317>
 - [38] Jose B. Pereira-Leal, Anton J. Enright, and Christos A. Ouzounis. 2003. Detection of functional modules from protein interaction networks. *Proteins: Structure, Function, and Bioinformatics* 54, 1 (9 2003), 49–57. <https://doi.org/10.1002/prot.10505>
 - [39] Bryan Perozzi, Rami Al-Rfou, and Steven Skiena. 2014. DeepWalk: online learning of social representations. In *Proceedings of the 20th ACM SIGKDD international conference on Knowledge discovery and data mining - KDD '14*. ACM Press, New York, New York, USA, 701–710. <https://doi.org/10.1145/2623330.2623732>
 - [40] Xinyu Que, Fabio Checconi, Fabrizio Petrini, and John A. Gunnels. 2015. Scalable Community Detection with the Louvain Algorithm. In *2015 IEEE International Parallel and Distributed Processing Symposium*. IEEE, 28–37. <https://doi.org/10.1109/IPDPS.2015.59>
 - [41] Usha Nandini Raghavan, Réka Albert, and Soundar Kumara. 2007. Near linear time algorithm to detect community structures in large-scale networks. *Physical Review E* 76, 3 (9 2007), 036106. <https://doi.org/10.1103/PhysRevE.76.036106>
 - [42] Georgios Rizos, Symeon Papadopoulos, and Yiannis Kompatsiaris. 2017. Multilabel user classification using the community structure of online networks. *PLOS ONE* 12, 3 (2017), e0173347. <https://doi.org/10.1371/journal.pone.0173347>

- [43] Ryan A Rossi and Nesreen K Ahmed. 2015. The Network Data Repository with Interactive Graph Analytics and Visualization. In *Proceedings of the Twenty-Ninth AAAI Conference on Artificial Intelligence*. AAAI Press, Austin, Texas. <http://networkrepository.com/>
- [44] Natalie Stanley, Roland Kwitt, Marc Niethammer, and Peter J. Mucha. 2018. Compressing Networks with Super Nodes. *Scientific Reports* 8, 1 (12 2018), 10892. <https://doi.org/10.1038/s41598-018-29174-3>
- [45] Ahsen J. Uppal and H. Howie Huang. 2018. Fast Stochastic Block Partition for Streaming Graphs. In *2018 IEEE High Performance Extreme Computing Conference (HPEC)*. IEEE, 1–6. <https://doi.org/10.1109/HPEC.2018.8547523>
- [46] Ahsen J. Uppal, Guy Swope, and H. Howie Huang. 2017. Scalable stochastic block partition. In *2017 IEEE High Performance Extreme Computing Conference (HPEC)*. IEEE, 1–5. <https://doi.org/10.1109/HPEC.2017.8091050>
- [47] Stéfan van der Walt, S Chris Colbert, and Gaël Varoquaux. 2011. The NumPy Array: A Structure for Efficient Numerical Computation. *Computing in Science & Engineering* 13, 2 (3 2011), 22–30. <https://doi.org/10.1109/MCSE.2011.37>
- [48] Tianyi Wang, Yang Chen, Zengbin Zhang, Tianyin Xu, Long Jin, Pan Hui, Beixing Deng, and Xing Li. 2011. Understanding graph sampling algorithms for social network analysis. In *Proceedings - International Conference on Distributed Computing Systems*. <https://doi.org/10.1109/ICDCSW.2011.34>
- [49] Frank Wanye, Vitaliy Gleyzer, and Wu-chun Feng. 2019. Fast Stochastic Block Partitioning via Sampling. In *2019 IEEE High Performance Extreme Computing Conference (HPEC)*. IEEE, Waltham, MA, USA, 1–7. <https://doi.org/10.1109/HPEC.2019.8916542>
- [50] Darren J Wilkinson. 2005. Parallel Bayesian Computation. In *Handbook of Parallel Computing and Statistics* (1st ed.), Erricos John Kontogiorghe (Ed.). Marcel Dekker/CRC Press, Boca Raton, Florida; London, UK, Chapter 18, 481–512. <http://www.mas.ncl.ac.uk/~ndjw1/docs/psc.pdf>
- [51] Jaewon Yang and Jure Leskovec. 2012. Community-Affiliation Graph Model for Overlapping Network Community Detection. In *2012 IEEE 12th International Conference on Data Mining*. IEEE, 1170–1175. <https://doi.org/10.1109/ICDM.2012.139>
- [52] Jaewon Yang and Jure Leskovec. 2015. Defining and evaluating network communities based on ground-truth. *Knowledge and Information Systems* 42, 1 (1 2015), 181–213. <https://doi.org/10.1007/s10115-013-0693-z>

A SYNTHETIC GRAPH RESULTS

A.1 F1 Score Results

Table 3 shows the average F1 scores obtained for each graph by each sampling algorithm, including the baseline (None). In 24 out of the 31 graphs, the difference between the F1 scores obtained with our sampling approach and the baseline is greater than or equal to -0.05 . On the graph where our approach performs worst when compared to the baseline, S30, we can still obtain an F1 score difference of just 0.06.

Table 3. Average F1 Scores for synthetic graph experiments

| Graph ID | None | 50% Sample Size | | | | | 30% Sample Size | | | | | 10% Sample Size | | | | |
|----------|-------------|-----------------|------|-------------|-------------|------|-----------------|------|-------------|-------------|------|-----------------|------|-------------|------|------|
| | | ES | FF | MD | RNN | UR | ES | FF | MD | RNN | UR | ES | FF | MD | RNN | UR |
| S1 | 0.54 | 0.51 | 0.49 | 0.54 | 0.51 | 0.50 | 0.50 | 0.38 | 0.52 | 0.51 | 0.31 | 0.40 | 0.08 | 0.49 | 0.39 | 0.04 |
| S2 | 0.58 | 0.53 | 0.51 | 0.55 | 0.53 | 0.49 | 0.50 | 0.34 | 0.53 | 0.51 | 0.32 | 0.42 | 0.06 | 0.50 | 0.41 | 0.04 |
| S3 | 0.59 | 0.51 | 0.50 | 0.54 | 0.52 | 0.50 | 0.48 | 0.32 | 0.52 | 0.52 | 0.30 | 0.44 | 0.05 | 0.51 | 0.43 | 0.03 |
| S4 | 0.62 | 0.55 | 0.50 | 0.56 | 0.54 | 0.51 | 0.49 | 0.28 | 0.55 | 0.54 | 0.27 | 0.40 | 0.04 | 0.51 | 0.41 | 0.02 |
| S5 | 0.59 | 0.56 | 0.51 | 0.57 | 0.56 | 0.49 | 0.49 | 0.28 | 0.54 | 0.53 | 0.26 | 0.40 | 0.04 | 0.51 | 0.44 | 0.02 |
| S6 | 0.60 | 0.57 | 0.48 | 0.58 | 0.57 | 0.48 | 0.50 | 0.21 | 0.54 | 0.53 | 0.23 | 0.39 | 0.03 | 0.51 | 0.44 | 0.02 |
| S7 | 0.55 | 0.67 | 0.65 | 0.68 | 0.66 | 0.65 | 0.65 | 0.50 | 0.65 | 0.65 | 0.51 | 0.60 | 0.25 | 0.65 | 0.59 | 0.20 |
| S8 | 0.59 | 0.62 | 0.58 | 0.62 | 0.60 | 0.57 | 0.58 | 0.43 | 0.60 | 0.60 | 0.44 | 0.55 | 0.12 | 0.60 | 0.56 | 0.08 |
| S9 | 0.58 | 0.57 | 0.53 | 0.58 | 0.56 | 0.53 | 0.50 | 0.35 | 0.54 | 0.55 | 0.32 | 0.44 | 0.06 | 0.53 | 0.45 | 0.04 |
| S10 | 0.51 | 0.46 | 0.42 | 0.48 | 0.45 | 0.42 | 0.39 | 0.24 | 0.44 | 0.42 | 0.19 | 0.32 | 0.03 | 0.40 | 0.33 | 0.02 |
| S11 | 0.41 | 0.34 | 0.32 | 0.36 | 0.35 | 0.32 | 0.28 | 0.14 | 0.34 | 0.31 | 0.11 | 0.21 | 0.02 | 0.30 | 0.16 | 0.01 |
| S12 | 0.58 | 0.54 | 0.50 | 0.55 | 0.54 | 0.49 | 0.49 | 0.31 | 0.51 | 0.51 | 0.33 | 0.42 | 0.04 | 0.50 | 0.41 | 0.02 |
| S13 | 0.56 | 0.53 | 0.49 | 0.54 | 0.53 | 0.50 | 0.48 | 0.29 | 0.52 | 0.51 | 0.29 | 0.38 | 0.05 | 0.50 | 0.43 | 0.03 |
| S14 | 0.56 | 0.54 | 0.50 | 0.56 | 0.52 | 0.50 | 0.50 | 0.31 | 0.52 | 0.51 | 0.29 | 0.39 | 0.05 | 0.50 | 0.44 | 0.03 |
| S15 | 0.58 | 0.55 | 0.50 | 0.57 | 0.53 | 0.51 | 0.49 | 0.32 | 0.53 | 0.51 | 0.32 | 0.43 | 0.06 | 0.50 | 0.41 | 0.04 |
| S16 | 0.60 | 0.57 | 0.53 | 0.60 | 0.54 | 0.51 | 0.50 | 0.34 | 0.55 | 0.53 | 0.31 | 0.41 | 0.06 | 0.54 | 0.44 | 0.04 |
| S17 | 0.13 | 0.33 | 0.33 | 0.36 | 0.33 | 0.33 | 0.20 | 0.16 | 0.30 | 0.22 | 0.15 | 0.31 | 0.01 | 0.16 | 0.02 | 0.01 |
| S18 | 0.41 | 0.49 | 0.47 | 0.51 | 0.47 | 0.47 | 0.44 | 0.29 | 0.42 | 0.46 | 0.29 | 0.38 | 0.04 | 0.45 | 0.36 | 0.02 |
| S19 | 0.56 | 0.55 | 0.49 | 0.56 | 0.53 | 0.51 | 0.49 | 0.34 | 0.52 | 0.51 | 0.33 | 0.42 | 0.05 | 0.50 | 0.39 | 0.03 |
| S20 | 0.61 | 0.54 | 0.53 | 0.57 | 0.55 | 0.52 | 0.51 | 0.34 | 0.55 | 0.54 | 0.33 | 0.44 | 0.07 | 0.51 | 0.44 | 0.03 |
| S21 | 0.66 | 0.59 | 0.58 | 0.60 | 0.58 | 0.56 | 0.54 | 0.39 | 0.56 | 0.54 | 0.37 | 0.49 | 0.09 | 0.52 | 0.46 | 0.04 |
| S22 | 0.41 | 0.51 | 0.51 | 0.53 | 0.50 | 0.50 | 0.47 | 0.32 | 0.46 | 0.49 | 0.30 | 0.45 | 0.05 | 0.49 | 0.38 | 0.03 |
| S23 | 0.47 | 0.51 | 0.49 | 0.54 | 0.50 | 0.49 | 0.47 | 0.33 | 0.49 | 0.48 | 0.33 | 0.44 | 0.05 | 0.48 | 0.41 | 0.03 |
| S24 | 0.57 | 0.52 | 0.51 | 0.55 | 0.52 | 0.51 | 0.48 | 0.31 | 0.48 | 0.49 | 0.30 | 0.41 | 0.05 | 0.48 | 0.41 | 0.03 |
| S25 | 0.61 | 0.55 | 0.52 | 0.57 | 0.54 | 0.51 | 0.49 | 0.31 | 0.56 | 0.52 | 0.31 | 0.42 | 0.05 | 0.51 | 0.43 | 0.03 |
| S26 | 0.63 | 0.55 | 0.51 | 0.57 | 0.54 | 0.53 | 0.50 | 0.35 | 0.56 | 0.54 | 0.32 | 0.46 | 0.04 | 0.52 | 0.42 | 0.03 |
| S27 | 0.24 | 0.55 | 0.54 | 0.59 | 0.55 | 0.55 | 0.49 | 0.43 | 0.56 | 0.49 | 0.42 | 0.28 | 0.14 | 0.21 | 0.12 | 0.09 |
| S28 | 0.87 | 0.72 | 0.57 | 0.81 | 0.80 | 0.57 | 0.55 | 0.36 | 0.81 | 0.64 | 0.36 | 0.33 | 0.11 | 0.39 | 0.28 | 0.11 |
| S29 | 0.90 | 0.73 | 0.58 | 0.84 | 0.83 | 0.58 | 0.54 | 0.40 | 0.83 | 0.71 | 0.39 | 0.38 | 0.07 | 0.41 | 0.37 | 0.06 |
| S30 | 0.89 | 0.74 | 0.63 | 0.85 | 0.85 | 0.62 | 0.57 | 0.46 | 0.86 | 0.75 | 0.46 | 0.44 | 0.08 | 0.49 | 0.44 | 0.07 |
| S31 | 0.91 | 0.76 | 0.67 | 0.85 | 0.84 | 0.66 | 0.62 | 0.53 | 0.85 | 0.77 | 0.53 | 0.48 | 0.05 | 0.56 | 0.52 | 0.06 |

A.2 Speedup Results

Table 4 shows the speedups obtained for each graph by each sampling algorithm over the baseline. Uniform Random (UR) and Forest Fire (FF) sampling always achieve the best speedups, due to the fast sampling time and lower density of the resulting sampled graphs. However, the quality of community detection results obtained with these algorithms is low. Of the remaining 3 algorithms, Random Node Neighbor (RNN) sampling results in the best speedups at the 50% sample sizes, though Expansion Snowball (ES) is faster at the 30% and 10% sample sizes.

Table 4. Average speedup for synthetic graph experiments

| Graph ID | 50% Sample Size | | | | | 30% Sample Size | | | | | 10% Sample Size | | | | |
|----------|-----------------|-------------|------|------|-------------|-----------------|--------------|------|------|--------------|-----------------|--------------|-------|-------|--------------|
| | ES | FF | MD | RNN | UR | ES | FF | MD | RNN | UR | ES | FF | MD | RNN | UR |
| S1 | 1.60 | 2.28 | 1.99 | 2.12 | 2.37 | 4.30 | 5.07 | 3.14 | 3.81 | 5.28 | 10.03 | 11.74 | 8.33 | 10.09 | 14.40 |
| S2 | 1.32 | 2.24 | 1.86 | 2.00 | 2.31 | 4.11 | 5.24 | 3.22 | 4.01 | 5.31 | 10.74 | 13.73 | 9.01 | 11.57 | 13.47 |
| S3 | 1.09 | 2.20 | 1.84 | 2.01 | 2.32 | 3.94 | 5.13 | 3.09 | 3.81 | 5.25 | 11.27 | 15.33 | 9.01 | 11.95 | 13.95 |
| S4 | 0.95 | 2.42 | 1.93 | 2.13 | 2.47 | 4.39 | 6.05 | 3.53 | 4.44 | 6.20 | 11.78 | 17.14 | 9.50 | 13.47 | 16.48 |
| S5 | 0.61 | 2.41 | 1.86 | 2.03 | 2.42 | 3.94 | 5.59 | 3.17 | 4.02 | 5.81 | 10.82 | 17.36 | 8.69 | 12.86 | 14.07 |
| S6 | 0.43 | 2.55 | 1.94 | 2.10 | 2.53 | 3.74 | 6.13 | 3.07 | 4.02 | 5.98 | 11.40 | 19.95 | 9.18 | 14.24 | 16.99 |
| S7 | 1.24 | 2.36 | 1.98 | 2.09 | 2.39 | 3.96 | 5.74 | 3.21 | 3.93 | 5.68 | 12.28 | 20.84 | 9.47 | 13.90 | 19.49 |
| S8 | 1.18 | 2.44 | 1.97 | 2.21 | 2.44 | 4.25 | 5.77 | 3.33 | 4.16 | 5.78 | 12.47 | 18.60 | 10.04 | 14.45 | 18.22 |
| S9 | 1.05 | 2.27 | 1.86 | 2.04 | 2.36 | 4.00 | 5.39 | 3.16 | 4.08 | 5.46 | 11.50 | 15.51 | 8.94 | 12.71 | 14.87 |
| S10 | 1.03 | 2.38 | 1.95 | 2.13 | 2.44 | 4.27 | 5.44 | 3.35 | 4.20 | 5.52 | 11.17 | 14.56 | 9.25 | 11.95 | 12.92 |
| S11 | 1.16 | 2.55 | 2.04 | 2.34 | 2.68 | 4.76 | 5.86 | 3.63 | 4.66 | 5.94 | 10.85 | 14.21 | 9.46 | 11.19 | 12.33 |
| S12 | 1.10 | 2.38 | 2.00 | 2.08 | 2.49 | 4.40 | 5.61 | 3.42 | 4.32 | 5.67 | 11.99 | 14.95 | 9.07 | 13.67 | 14.65 |
| S13 | 1.09 | 2.40 | 1.97 | 2.15 | 2.52 | 4.38 | 5.50 | 3.39 | 4.28 | 5.49 | 12.33 | 16.59 | 9.35 | 13.08 | 15.46 |
| S14 | 1.10 | 2.37 | 1.93 | 2.10 | 2.43 | 4.28 | 5.51 | 3.32 | 4.20 | 5.61 | 11.79 | 15.86 | 9.33 | 13.32 | 15.41 |
| S15 | 1.01 | 2.23 | 1.88 | 2.03 | 2.35 | 3.97 | 5.27 | 3.17 | 4.02 | 5.42 | 11.71 | 15.73 | 9.24 | 12.79 | 14.63 |
| S16 | 1.10 | 2.30 | 1.90 | 2.06 | 2.37 | 4.29 | 5.82 | 3.40 | 4.25 | 5.89 | 11.94 | 16.77 | 9.03 | 12.76 | 16.42 |
| S17 | 1.20 | 2.29 | 1.83 | 2.00 | 2.26 | 4.31 | 5.19 | 3.24 | 4.09 | 5.16 | 10.52 | 25.31 | 9.02 | 14.78 | 24.70 |
| S18 | 1.20 | 2.43 | 2.01 | 2.17 | 2.57 | 4.48 | 5.80 | 3.57 | 4.29 | 5.59 | 12.44 | 17.15 | 9.70 | 13.76 | 16.47 |
| S19 | 1.09 | 2.39 | 2.04 | 2.15 | 2.50 | 4.47 | 5.87 | 3.49 | 4.42 | 5.82 | 12.47 | 16.87 | 10.17 | 13.50 | 15.66 |
| S20 | 1.07 | 2.44 | 1.97 | 2.14 | 2.47 | 4.28 | 5.56 | 3.43 | 4.30 | 5.75 | 12.13 | 16.02 | 9.80 | 12.99 | 14.85 |
| S21 | 1.00 | 2.25 | 1.89 | 2.04 | 2.33 | 4.15 | 5.40 | 3.38 | 4.14 | 5.47 | 12.14 | 15.28 | 9.95 | 13.34 | 14.20 |
| S22 | 0.98 | 2.29 | 2.04 | 2.15 | 2.36 | 4.39 | 5.52 | 3.54 | 4.37 | 5.52 | 12.92 | 17.07 | 10.01 | 14.23 | 14.39 |
| S23 | 0.94 | 2.19 | 1.93 | 2.07 | 2.29 | 4.07 | 5.19 | 3.36 | 3.94 | 5.24 | 11.81 | 15.69 | 9.40 | 13.20 | 14.25 |
| S24 | 1.03 | 2.39 | 1.92 | 2.11 | 2.42 | 4.25 | 5.66 | 3.43 | 4.24 | 5.50 | 12.12 | 16.85 | 9.72 | 13.41 | 15.40 |
| S25 | 1.16 | 2.26 | 1.85 | 2.04 | 2.33 | 4.22 | 5.51 | 3.34 | 4.16 | 5.60 | 11.94 | 15.94 | 8.81 | 13.01 | 15.19 |
| S26 | 1.16 | 2.30 | 1.78 | 2.01 | 2.36 | 4.19 | 5.43 | 3.32 | 4.08 | 5.44 | 11.39 | 16.26 | 8.68 | 12.68 | 15.18 |
| S27 | 2.17 | 2.45 | 1.93 | 2.18 | 2.54 | 4.34 | 5.79 | 3.34 | 4.44 | 6.05 | 11.60 | 12.54 | 9.60 | 12.19 | 12.04 |
| S28 | 2.24 | 4.68 | 1.17 | 1.35 | 4.75 | 4.78 | 11.82 | 1.68 | 2.86 | 11.99 | 14.97 | 21.21 | 9.58 | 16.19 | 20.81 |
| S29 | 2.73 | 6.08 | 1.28 | 1.44 | 6.11 | 7.63 | 17.46 | 1.97 | 3.20 | 18.33 | 23.62 | 30.91 | 12.09 | 23.73 | 34.28 |
| S30 | 3.06 | 5.76 | 1.17 | 1.40 | 5.62 | 8.10 | 19.87 | 1.79 | 2.90 | 19.85 | 25.07 | 37.57 | 11.99 | 24.67 | 36.39 |
| S31 | 3.44 | 6.76 | 1.28 | 1.48 | 7.05 | 10.57 | 23.73 | 1.98 | 3.12 | 23.88 | 30.17 | 45.28 | 11.57 | 25.00 | 43.82 |

A.3 Results on the Sampled Graph

In this section, we compare 3 different F1 Score measures:

- (1) $F1(\text{Baseline})$: The F1 Score calculated on the vertex-to-community assignment obtained via running the baseline algorithm on the entire graph
- (2) $F1(\text{Sampling})$: The F1 Score calculated on the vertex-to-community assignment obtained via running our sampling approach

- (3) $F1(\text{Partial})$: The F1 Score calculated on the partial vertex-to-community assignment obtained via running SBP on only the sampled portion of the graph (see Step 2 of our sampling approach in §3.1).

Our results (see Fig. 16) show that $F1(\text{Partial})$ is almost always higher than $F1(\text{Sampling})$. This is intuitive because if the sampled graph does not adequately sample any communities, those communities will be missing from the results on the full graph. A more interesting observation is that $F1(\text{Partial})$ is also higher $F1(\text{Baseline})$. This effect may be due to the sampled graph having more clearly delineated communities, or it may be an artifact of the reduced search space due to sampling. We consider a more definitive analysis beyond the scope of this manuscript, and leave it to future work. Note that this effect is not observed with the two worst-performing sampling algorithms: Forest Fire (FF) and Uniform Random (UR) sampling.

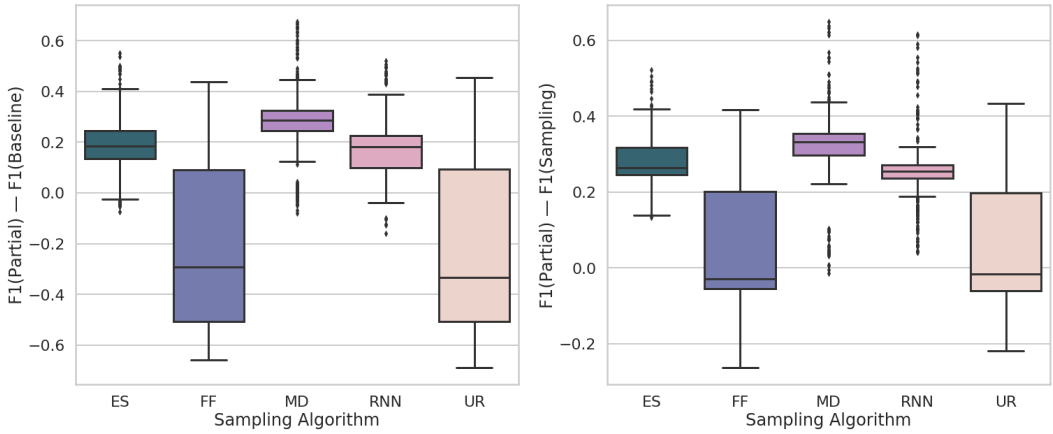


Fig. 16. Comparison of F1 scores on the sampled graph with (left) the F1 scores obtained by the baseline algorithm on the full graph, and (right) the F1 scores obtained with sampling on the full graph. In both cases, Maximum Degree (MD), Random Node Neighbor (RNN) and Expansion Snowball (ES) sampling routinely lead to better F1 scores on the sampled graph than on the full graph.

B WEB GRAPH RESULTS

B.1 Quality Score Results

Table 5 shows the average Quality Scores obtained for each graph by each sampling algorithm at the 30% sample size, including the baseline (None). In 6 out of the 10 graphs, Maximum Degree (MD) sampling results in the highest Quality Scores. However, the quality scores on all graphs except R10 are close, suggesting that the solutions obtained with all 3 sampling algorithms are similar in how well they describe the graph. On R10, Expansion Snowball (ES) sampling outperforms the other two sampling algorithms by a wide margin. Note that all the Quality Scores obtained with our sampling approach are very close, and 4 cases even match the scores obtained by the baseline, showing very good quality preservation.

B.2 Speedup Results

Table 6 shows the average speedup obtained on each web graph by each sampling algorithm at the 30% sample size. The algorithm that produces the highest speedup is always either the Random

Table 5. Average quality scores for real-world graph experiments.

| Graph ID | None | ES | MD | RNN |
|----------|-------------|-------------|-------------|-------------|
| R1 | 0.67 | 0.66 | 0.66 | 0.66 |
| R2 | 0.68 | 0.65 | 0.66 | 0.65 |
| R3 | 0.66 | 0.64 | 0.65 | 0.65 |
| R4 | 0.72 | 0.69 | 0.70 | 0.71 |
| R5 | 0.68 | 0.65 | 0.68 | 0.67 |
| R6 | 0.45 | 0.42 | 0.45 | 0.44 |
| R7 | 0.56 | 0.55 | 0.56 | 0.56 |
| R8 | 0.68 | 0.66 | 0.68 | 0.66 |
| R9 | 0.70 | 0.67 | 0.69 | 0.69 |
| R10 | 0.84 | 0.83 | 0.54 | 0.61 |

Node Neighbor (RNN) or the Expansion Snowball (ES) algorithm, which is consistent with the results obtained on synthetic graphs. The greatest speedup obtained is 20.58 \times on R10 using ES sampling.

Table 6. Average speedup for real-world graph experiments.

| Graph ID | ES | MD | RNN |
|----------|--------------|------|-------------|
| R1 | 2.50 | 2.45 | 2.68 |
| R2 | 2.78 | 2.19 | 2.30 |
| R3 | 2.77 | 2.17 | 3.69 |
| R4 | 2.49 | 1.73 | 2.92 |
| R5 | 3.28 | 1.97 | 2.43 |
| R6 | 3.47 | 2.91 | 3.25 |
| R7 | 2.78 | 2.97 | 3.80 |
| R8 | 4.28 | 1.16 | 1.17 |
| R9 | 3.55 | 2.20 | 3.60 |
| R10 | 20.58 | 3.84 | 5.75 |